Compact 4 × 4 Butler matrix design-based switch beamforming antenna array for 5G applications

Ali Abdulateef Abdulbari[1], Sharul Kamal Abdul Rahim[1], Tan KIM GEOK[2], Amna shibib kamel[3], Raya adil kamil[3], Hatem Oday Hanoosh[4], and Mustafa Mohammed Jawad[3]

[1]Universiti Teknologi Malaysia Wireless Communication Centre
[2]Multimedia University Faculty of Engineering and Technology
[3]Al-Turath University College
[4]Imam Ja'afar Al-Sadiq University

May 3, 2023

Abstract

This paper, presents a 4×4 BM based on four direction switch BM antenna array. The proposed design operated at 3.5 GHz. The use of multi-beam antennas or switched-beam antenna arrays (SAAs) promised users of high-gain and large coverage areas for 5G technologies. The BM was implemented by combining 3-dB BLC, two crossovers, and 45 ^{o} phase shifters fabricated on the RT5880LZ substrate, with using a triangular slot and T-shape based on the BM design. The proposed design focused on the miniaturization and enhancement of the bandwidth. The return loss and isolation were better than -15 dB at all the ports, according to the simulated and measured result showed that with excellent insertion loss -6.1 ± 2 dB. A fractional bandwidth of 49.7% and the overall dimension were reduced to 56% as compared to the conventional BLC and crossover. Hence, the proposed design of BM performed an excellent size reduction of 80% and improvement bandwidth up to 836 MHz compared to the traditional BM. The switched beam directions were measured at -34 ^{o}, -40 ^{o}, +32 ^{o} and +35 ^{o} at 3.5 GHz for each input port of 1-4 excitation. The proposed design BM is suitable of 5G application.

Compact 4 × 4 Butler matrix design-based switch beamforming antenna array for 5G applications

Ali Abdulateef Abdulbari * [1,1,2], Sharul Kamal Abdul Rahim [2,1], Tan KIM GEOK[3] , Amna shibib kamel [4,2], Raya adil kamil[5,2], Hatem Oday Hanoosh[4,6] ,Mustafa Mohammed Jawad[7,2]

[1]Wireless Communication Centre (WCC), School of Electrical Engineering, Universiti Teknologi Malaysia (UTM), Skudai 81310, Malaysia.

[2]Department of Medical Devices Techniques Engineering, Al-Turath University College, Baghdad, Iraq.

[3]Faculty of Engineering and Technology, Multimedia University, Melaka 75450, Malaysia.

[4]Department of Computer Techniques Engineering, College of Information Technology, Imam Ja'afar Al Sadiq University,Samawah, Iraq.

ABSTRACT

This paper, presents a 4×4 BM based on four direction switch BM antenna array. The proposed design operated at 3.5 GHz. The use of multi-beam antennas or switched-beam antenna arrays (SAAs) promised users of high-gain and large coverage areas for 5G technologies. The BM was implemented by combining 3-dB BLC, two crossovers, and 45^o phase shifters fabricated on the RT5880LZ substrate, with using a triangular slot and T-shape based on the BM design. The proposed design focused on the miniaturization and enhancement of the bandwidth. The return loss and isolation were better than -15 dB at all the ports, according to the simulated and measured result showed that with excellent insertion loss -6.1 ± 2 dB. A fractional bandwidth of 49.7% and the overall dimension were reduced to 56% as compared to the conventional BLC and crossover. Hence, the proposed design of BM performed an excellent size reduction of 80% and improvement bandwidth up to 836 MHz compared to the traditional BM. The switched beam directions were measured at -34°, -40°, +32° and +35° at 3.5 GHz for each input port of 1-4 excitation. The proposed design BM is suitable of 5G application.

Keyword: Beamforing, Butler matrix, antenna array, 5G, triangular slot, T-shape, branch line coupler (BLC), microstrip antenna, antenna array.

IntroductionThe demand for wireless technology is substantially increasing because of the rapid growth of wireless technological innovations. Currently, several billion wireless-electronic devices are linked to the internet network, and these figures are expected to rise in the coming years. So, researchers have started to put tremendous effort in the area of 5G technology[1][2][3]. The deployment of 5G wireless, as well as the current and upcoming Beyond 5G (B5G) communication system, point towards a revolutionary change in modern-day telecommunications, leading to a complete paradigm shift in the way end-users will communicate in the coming years [4][5]. Meanwhile, the number of co-channel interference users will increase and improve the inferior quality of service [6][7]. In the development of 5G systems, it is envisaged that switched-beam antenna arrays (SAAs) would play a vital role in obtaining the desired performance at the transceivers. This is the main objective sought by many researchers in the area of beam-forming network. Their focuses have always been on the problem and quality enhancement of the communication link [8]. Hence, the application of switch beam-forming networks (SBFNs) has always been the area of interest among researchers[9]. This technology significantly contributes to wider bandwidth and directional antenna array that can transfer and focus radiated power in the desired direction. It is widely applied in wireless communications [4]. The SBFNs are categorised into several types, such as Nolen matrix [10], Blass matrix [11], Rotman lens [12], and Butler matrix [13]. Butler matrix or BM is a popular technique due to its low cost, simple configuration, and low power dissipation. This technique is widely used in the filed beam-forming of antenna array [14]. BM is a passive device with multiple input and output ports. BM 4×4 consists of four 3-dB directional coupler, two phase shifters, and a crossover [15]. The beam-forming and beam-steering procedures are controlled by the BM design employing an antenna array. The signal-to-noise and clutter ratio is improved by the BM design's usage of frequency reuse [16]. In the last years, the BM 4×4 has been studied and improved in different ways, such as in [17] and for low loss [18]. The problem with conventional BM large size and narrow-band characteristics [19][20] is that these requirements are unable to meet the fifth generation (5G) application. However, to solve this issue, researchers have started to introduce a new design using many techniques to improve the Butler matrix[21]. The reported literature [22][23][24] has highlighted microstrip artificial transmission lines (ATLs) triangular slot, BM without crossover and phase shifter, and forward wave present in [25]. A reduced BM network has also been implemented at stub loaded TL, as well as presented and the multibeam antenna array has been validate. The size achieved for the Butler matrix was approximately 55% as compared to the traditional BM design [26]. Another way of using miniaturisation butler matrix design is through meandered line and dumbbell-shaped cross-slot technique based on the branch line coupler. The fractional BW was enhanced up to 37.5% and size miniaturised of 17% [27]. The coupler, crossover, and phase shifter sizes were reduced by BLC using artificial transmission lines, as in [28]. Recently, a triangular slot type artificial transmission line (ATL) has also been proposed. The artificial transmission line is, an easy-to-design, compact structure and easy to adjust electrical parameters, which is also helpful to build block for different microwave passive components [29]. The proposed 4 × 4 Butler matrix was design by using software Computer Simulation Technology (CST). This design utilised modified BLC, respectively. The BM Implementation was on the Rogers RT5880LZ with 0.25 mm thickness, relative permittivity εr=2, and loss tangent tanδ=0.002. Several BM designs that have been reported in previous work improved the bandwidth and size reduction. However, none of them attained bandwidth improvement and size reduction, together with an excellent performance for 5G beamforming network. Table 1 displays the specification design of the proposed designs. The novelty of this paper includes design of the BLC, crossover and BM by using triangular slot and T-shape structure, and antenna array based zig-zag shape.**Table 1. Specification**

of proposes designs.

Parameters	**Coupler**	**Crossover**	**Butler matrix**
Frequency	3.5 GHz	3.5 GHz	3.5 GHz
Technique	Triangular slot and T-shape	Triangular slot and T-shape	Triangular slot and T-shape
BW	1 GHz	1GHz	500 GHz
Phase difference	90°±1	0°	-45,135,-135,45
Insertion loss	-3dB±0.1	0dB	-6.1±2dB
S11	Below-10dB	Below -10dB	Below-10dB
S41	Below-10dB	Below -10dB	Below-10dB

Design of triangular slot The basic structure of the proposed microstrap artificial model transmission lines (ATL) with triangular slot is illustrated in Fig. 1(a). The equivalent circuit model of designed triangular slot patch BLC as illustrate in Fig. 1(b). The circuit model consists of combination inductors and capacitors both in series and parallel. We included an inductor and capacitors for the splits for the metal strip. The overall area of the triangular slot patch was approximated to that of the low impedance line in this case. The related parameters can be expressed as follows[30]:

$\mathrm{T}_{\mathrm{ATL}} = \left(\frac{L}{2}\right)^2$ (1) $\frac{L}{2} = \sqrt{2W_{\mathrm{TL}}L_{\mathrm{TL}}}$ (2)

Where TATL, L, WTL, and LTL, the width and length of the base line were ATL and TTL, respectively. In order to miniaturise the common 3-dB BLC, we proposed a triangular slot -type artificial model transmission lines with modified slots. This ATL was an isosceles triangular slot formed by folding a stepped impedance line (SIL) into a right angle, as shown in Fig.2 (a) Sex triangular slot BLC.

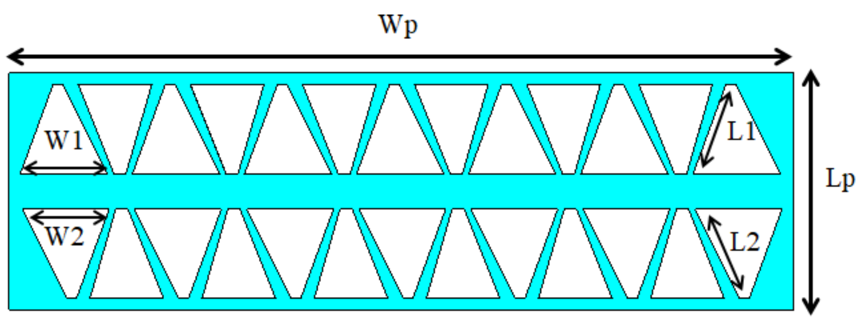

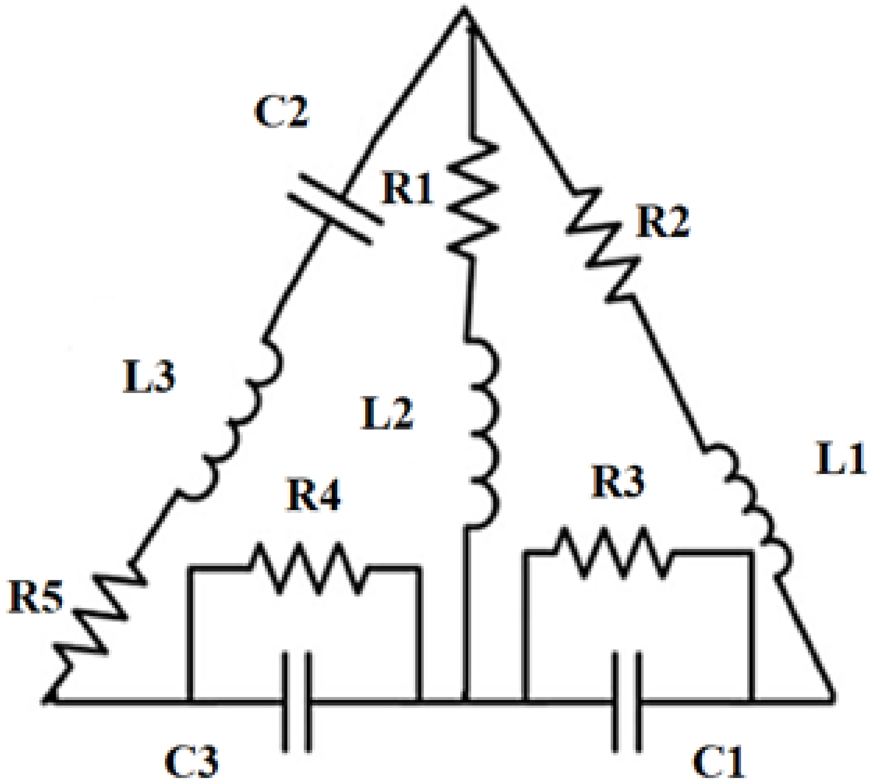

(b)

Fig. 1. (a) Geometry of basic (ATL) building (b) Lumped element equivalent circuit model of the design

The lumped equivalent circuit in Fig. 2 (d) to the impedance matrix [Z] 90° electrical lengths and certain characteristic impedance were used in the calculation for the first step of an ATL design.

[Z] =

$$\begin{bmatrix} \frac{Z_2\ (Z_3+Z_2)}{2Z_2+\ Z_3}\ Z_1 & \frac{Z_2^2}{2Z_2+\ Z_3} \\ \frac{Z_2^2}{2Z_2+\ Z_3} & \frac{Z_2\ (Z_3+Z_2)}{2Z_2+\ Z_3}\ Z_1 \end{bmatrix} \quad (3)$$

Where Z1 = jxL1, Z2 = -j/(wCb), Z3 = jwLc. L1,L2,L3 and w were the lumped element values in Fig. 2 (b) and angular frequency, respectivaly.The image impedance of the [Z], Z0, for the characteristic impedance of the ATL could then be calculated.

$Z_0 = \sqrt{z_{11}^2\ - z_{22}^2}$ (4)

From S22 was given as Eq.(5) and the component of S21 should be zero for any λ/4 transmission line of ϑ = 900, we could easily obtain the relation of Eq.(6) for a 900 artificial model transmission lines (ATL).

$S22 = \frac{2Z_{22}\ Z_T}{(Z_{11}+\ Z_{T)}\ (Z_{22}+\ Z_{T)-}\ Z_{22}\ Z_{21}} = |S_{21}|\, e^{j}$ (5)

Z1Z3 + (2Z1 + Z3) Z2 + Z23 = 0 (6)

How to design an ATL with a Z0 characteristic impedance an electrical length of 900. For the first step, we chose L and WTL x (x = 1, 2, and 3), considering the circuit size we needed, and obtained the LTL value using Eq. (1).

Branch line coupler

The proposed design BLC in this paper was a compact design based on microstrip artificial transmission lines (ATLs) with triangular slot patch and T-shape, as shown in Fig. 2, i.e., the coupler fabricated prototype. The horizontal and vertical TL's respective impedances were $Z0/\sqrt{2}$ and Z0, which were 35 and 50 . The width(W) and length(L) arms of the BLC could be calculated by using the equations in [31]. In our design, the chosen centre frequency of the proposed design was 3.5GHz. The optimised dimensions of the triangular slot ATL with 50 and 90^o electrical length were optimised as Wp = 14.00mm, W1=1.56 mm, W2= 1.31 mm, Wf = 4.0 mm, Wt = 0.40 mm, Wts = 0.30 mm, Wg = 0.21 mm, Wm = 1.2 mm, L1 = 1.78 mm, L2 = 1.66 mm, Lm = 13.8 mm, Lp = 4.23 mm, Lf = 1.5 mm, Lt = 4.80 mm, Lts = 4.10 mm, Lg = 0.75 mm, respectively. The dimensions for vertical and horizontal of the unit-call were optimised to achieve the BLC centre frequency of 3.5 GHz. The main component considered the BLC for the BM design. The proposed design coupler was simulated by)CST) microwave studio. Using the proposed design of the impedances, 3 dB BLC Eq.(7) and (8) were computed through the outputs phase difference = 90^o with Z0 = 50 , the value of the horizontal and vertical arms, which were Z1 = Z0 = 50 , Z2 = Z3 = 35.36 . Z1 = Z0 from Eq.12, which can be simplified as:

$Z_1 = Z_{0d}$ —sin [?] — (7)

$Z_2 = Z_3 = \frac{Z_o d\ sin}{\sqrt{1+\ d^2\ \ \sin^2}}$ (8)$\theta_1 = \frac{\pi}{}$

english2 (9)

θ_2=tan-1$\left(\frac{(Z_0 \tan)}{Z_1}\right)$(10)

θ_3=π–tan–1$\left(\frac{(Z_0 \tan)}{Z_1}\right)$(11)

θ_2 = tan-1 (tan[?]) [?] (12)

Where, is the phase difference at 3.5 GHz frequency and (d2) is the power division ration for the coupler. From Eq (7), for a given phase difference of BLC as 900, the electrical lengths were $\theta_2 = \theta_3$ = 900. The simulated and measured result for the return loss and phase difference to BLC are summarised in Fig. 2. The simulated in Fig. 2(a) to BLC operated between two bands for scattering parameter and isolation loss of 2.91GHz to 4.02GHz and 2.72GHz to 4.16 GHz. The results were below -10dB. The phase difference to the simulated between the output ports was found to be 900, as shown in Fig. 2(c).However, the measured result to BLC is as shown in Fig. 2(b) to the scattering parameter loss and isolation loss which operated between 2.62GHz to 2.5GHz. The phase difference to the measured between the output ports was found to be 87.50, as shown in Fig. 2(c). This small loss error at 3.6GHz due the SMA and coaxial cables. The insertion loss to the simulated and measured was also indicated in Fig.2 (a-b) -2±0.1dB and -3±0.2dB, respectively. There small difference between simulated and measured results for the proposed design BLC due fabricated and tools used. All of these measurements were carried out using Keysight (AgilentTechnologies) FieldFox N9925A vector network analyser (VNA). The λ/4 for the artificial transmission lines (ATLs) triangular slot patch provided good wide bandwidth and size reduction. The performance parameters such as return loss, insertion loss, isolation loss, and phase difference between output ports could be analysed with VNA. The BLC with dimension is as shown in Fig. 3(a), while the unused ports were terminated with 50 SMA terminator ports when the measurement took place, are illustrated in Fig. 3(b). Table 2 summarized to comparison the proposed design BLC with the previously published work.

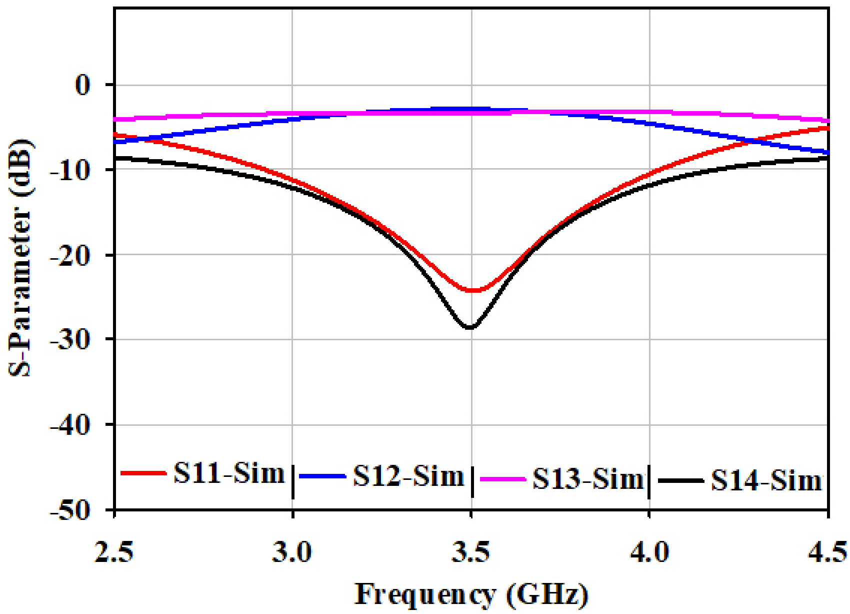
S-Parameter (dB)
0
-10
-20
-30
-40
-50
2.5
3.0
3.5
4.0
4.5
Frequency (GHz)
S11-Sim
S12-Sim
S13-Sim
S14-Sim

(a)

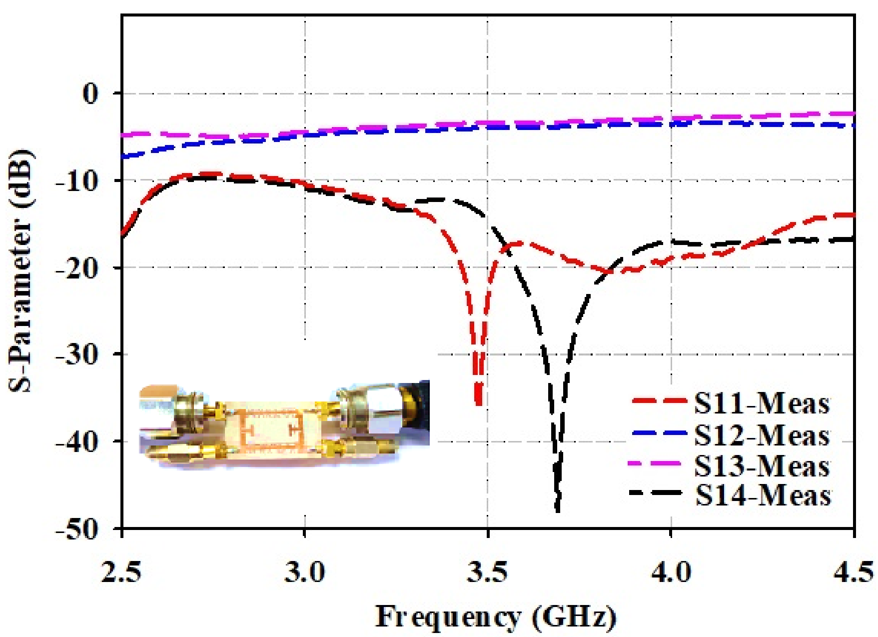
S-Parameter (dB)
0
-10
-20
-30
-40
-50
2.5
3.0
3.5
4.0
4.5
Frequency (GHz)
S11-Meas
S12-Meas
S13-Meas
S14-Meas

(b)

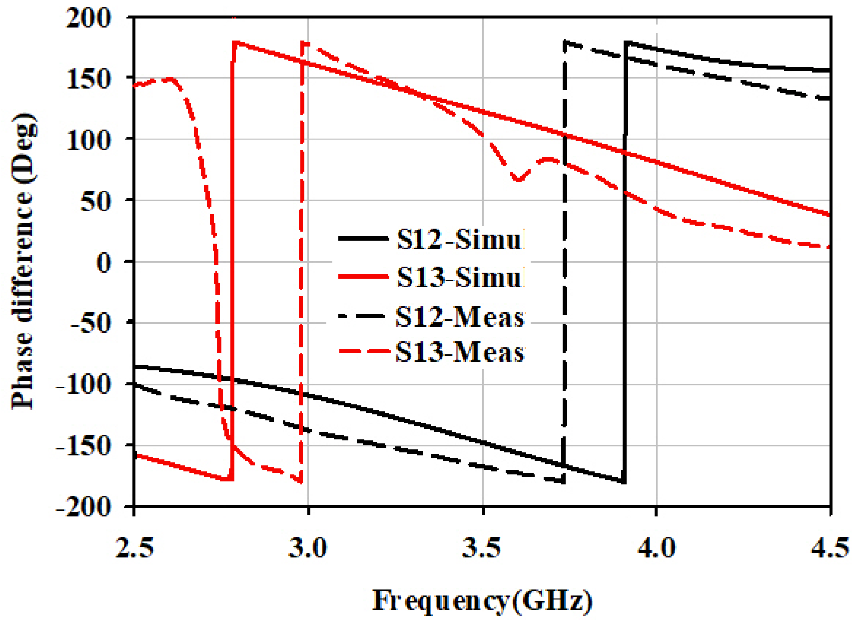

(c)

Fig. 2. (a) Simulated S-parameters result of the proposed BLC (b) Measured S-parameters result of the proposed BLC (c) Comparison between Simulated and measured Phase difference of BLC between two ports $S_{12}$and S_{13}.

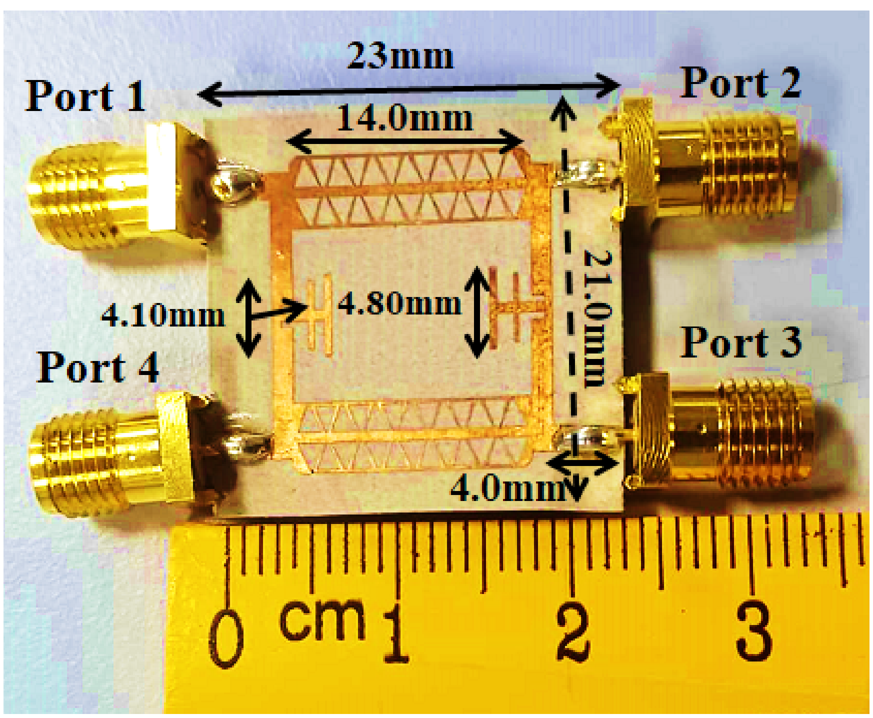

(a)

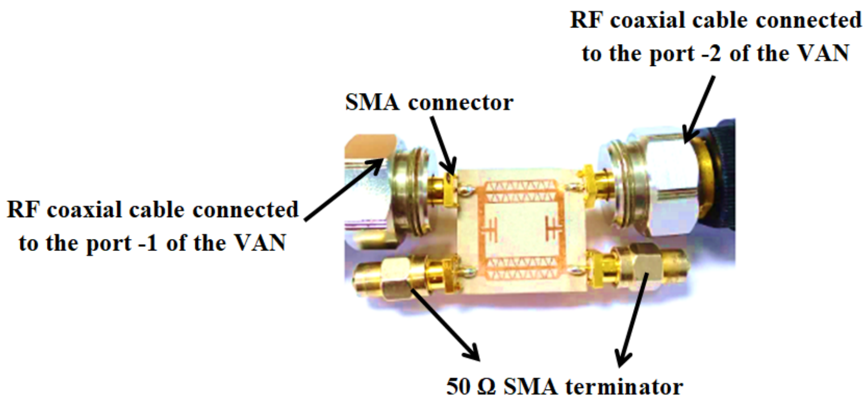

(b)

Fig. 3. (a) Fabricated of the proposed design BLC using substrate RT5880LZ, the BLC ports from 1-4, (b) The BLC under measurement with 50 SMA terminator.

Table. 2. C omparison between the Proposed BLC Design with previous work related

Ref.	**Type substrate**	**Operating** Freq. (GHz)	**Fractional** Bandwidth (S11 = -10dB)	**Size (mm × mm)**	**Loss Error (LE)** (dB)	**PD Error (Deg)**
[5]	FR-4	3.5	30.22%	27.2 × 16.5	± 0.9dB	-5°
[32]	Rogers RO4003	3.22	5%			

16.5 × 11.3

± 1dB

-3^{o}

[33]

FR-4

3.5

6.57%

23.5 × 17.5

± 1.7dB

-4^{o}

[34]

Rogers RT5880LZ

3.5

30.81%

22 × 24

± 0.9dB

-5^{o}

[35]

FR-4

3.5

14.6%

16 × 12

± 0.9dB

-1^{o}

[36]

Rogers RO4003

3.5

17%

10.5 × 15.5

± 0.5dB

-1.7^{o}

[This

work]

2023

Rogers RT5880LZ

3.5

33.34%

21.0 × 23.0

± 0.1dB

-1°

Crossover 0dB

The key feature of the crossover in BM is to avoid overlapping signals at crossings and maintain a reasonable level of isolation between signals at crossing lines. It means crossover allows two signals to cross each other while retaining a high degree of isolation [31]. The signal flowed to port 3 when port 1 was excited in contrast to the signal flowed to port 2 when port 4 was excited. Theoretically, crossover should be 0dB for the insertion loss. A 50 microstrip transmission line was used to design the crossover. It was fabricated by using a single layer Rogers RT5880LZ with relative permittivity (εr) 1.96, a thickness of 0.25mm, and loss tangent of 0.0009, respectively. The insertion loss S13 and S24 and as well as the phase difference S13 and S24 were implemented by compact two 3-dB BLC. The simulated return loss (S11) characteristics were achieved below -10dB within the range between 2.76GHz to 4.16GHz frequency band. For the selected compact design crossover for the development of the BM, the insertion loss to simulated and measured results were -0.16 dB and -0.5 dB, at the centre frequency of 3.5 GHz. The comparison between the S-parameters' response compact 0dB crossover is as shown in Fig. 4(a). Meanwhile, the phase differences between the simulated and measured results were similar to S13 and S24 is 0°, as shown in Fig. 4(b). The overall dimension for the fabricated of this work was 40mm × 21mm, as shown in Fig. 5(a).The proposed design under test of the S-parameters is illustrated in Fig. 5(b). The loss extra between simulated and measured induced by the SMA and coaxial cables.

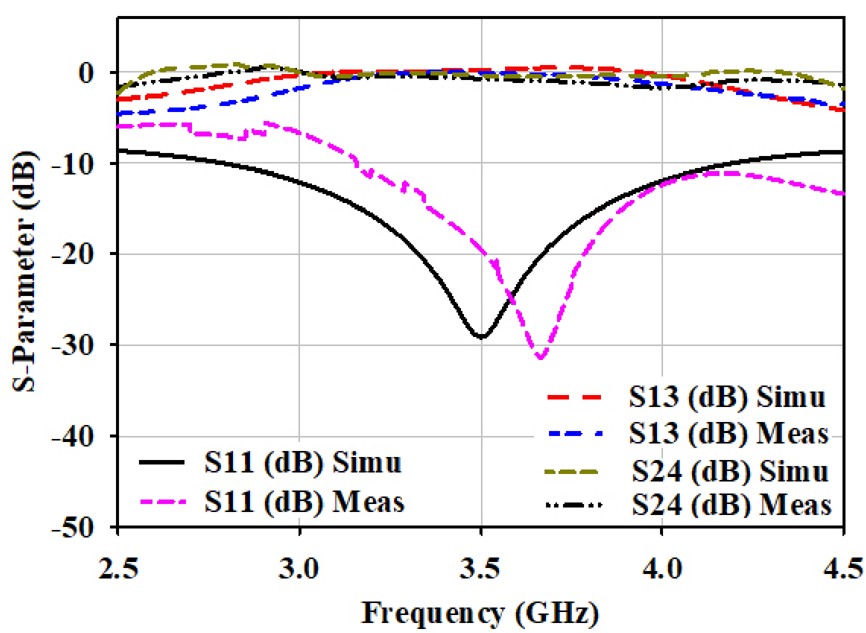

(a)

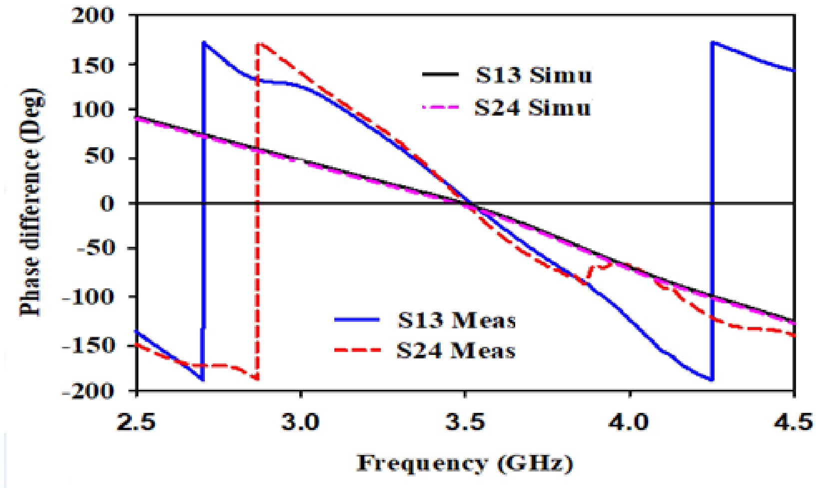

(b)

Fig. 4. (a) S-Parameters response of the crossover simulated and measured of the compact 0 dB (b) Phase different between simulated and measured of the compact 0 dB crossover.

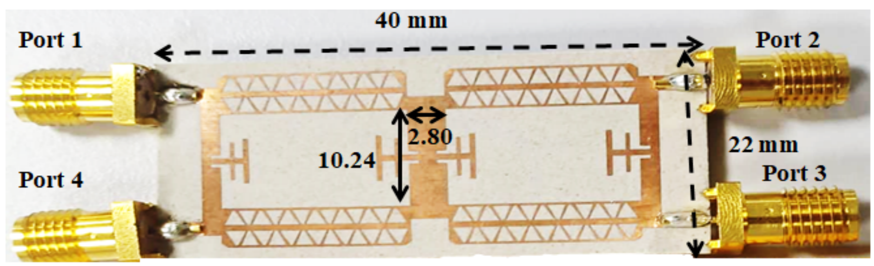

) a)

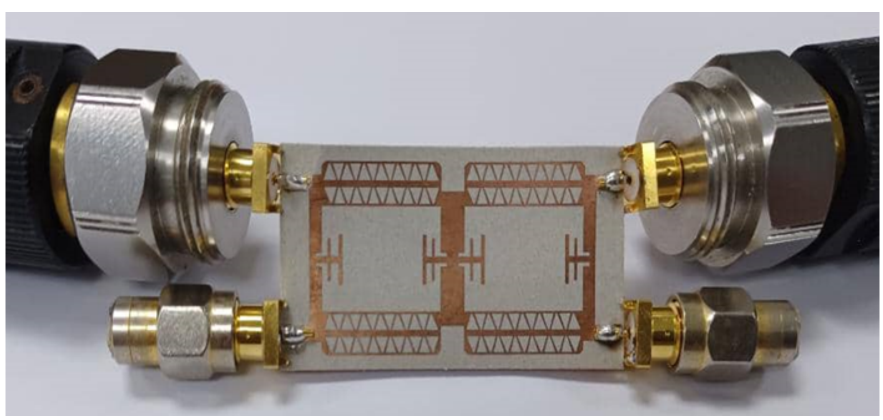

(b)

Fig. 5. (a) 0dB crossover fabricated by compact two 3-dB BLC with dimension using RT5880LZ substrate (b) The proposed design 0dB crossover under test.

Design configuration butler matrix

The proposed design of the 4 × 4 BM was conducted using a computer simulation technology (CST) microwave studio. The BM implementation was created using combined 3dB BLC of Triangular slot and T-shape, two crossover structures, and 45° phase shifter at the operate frequency of 3.5 GHz. The proposed design BM fabricated on a single layer of RT588LZ substrate. The final fabrication of the proposed BM design, which had the overall area of 87.5mm × 75mm, is as shown in Fig. 6.

The BM provided four outputs with equal amplitude and phase difference of -45°, 135°, 45°, and -135°, respectively. As a result, each input port, specifically as port 1, port 2, port 3, and port 4 were designated as port 5, port 6, port 7, and port 8, was able to produce four beams in various directions, as illustrated in Fig. 6. This configuration was of a 4 × 4 BM. Table 3 shows the phase shift that would be generated on each output based on the excited of the input ports, and all other ports were terminated at 50 loads. There were four cases. When input port 1 is excited the phase difference between the output ports -45°. The output 135deg phase difference when input port 2 is excited. The phase difference between the output ports in the third case will be -135° when input port 3 is excited. The last port phase difference of the output port is 45deg when input port 4 is excited. The proposed BM was validated in accordance with design criteria provided in Table 1.

Table 3. The phase difference between the outputs ports of the Butler matrix feed.

Ports	Output Port 5	Output Port 6	Output Port 7	Output Port 8
Input Port1	1350	900	450	00
Input Port 2	450	1800	-450	900
Input Port 3	900	-450	1800	-450
Input Port 4	00	450	900	1350
Phase Different Between Output ports	**-450**	**+1350**	**-1350**	**+450**

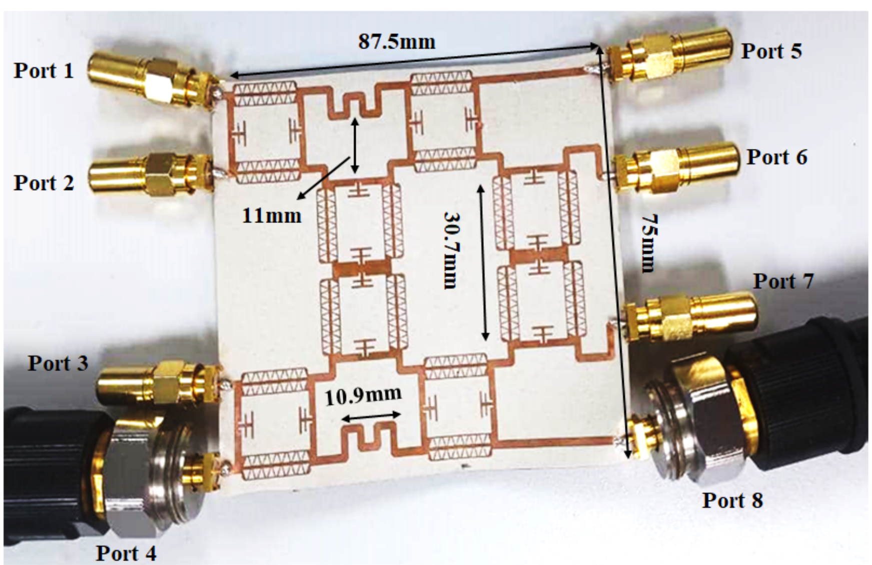

Fig.6.RT5880LZ substrate based fabricated prototype of the proposed 4×4 BM.

The simulated and measured S-parameters responses of the 4 × 4 Butler matrix result for different ports are as shown in Fig. 7, respectively. The P1 of the BM excited return loss was better than 17dB. This could be seen in the simulation and measured results of the return loss and insertion loss, which were S11 = -20.5 dB, S15 = -5.91 dB, S16 = -5.5 dB, S17 = -6.3 dB, S18 = -5.7 dB, and S11 = -18 dB, S15 = 6.41 dB, S16 = -5.6 dB, S17 = -5.8 dB, S18 = -6.0 dB, illustrate in Fig. 7(a - b). Hence, the average insertion loss for simulated and measured (S15,S16,S17,S18) were -5.9, 6.0 ± 2 dB, respectively. The P2 of the BM excited return loss was better than 14 dB. The simulation and measured results of the return loss and insertion loss were S22 = -25 dB, S25 = -6.35 dB, S26 = -6.4 dB, S27 = -5.43 dB, S28 = -5.85 dB, and S22 = -34 dB, S25 = -6.72 dB, S26 = -6.65 dB, S27 = -5.81 dB, S28 = -6.76 dB, as illustrated in Fig 7(c - d), The average insertion loss for simulated and measured (S25,S26,S27,S28) were -6.0, 6.5 ± 2, and dB, respectively. The P3 of the BM excited return loss was better than 10 dB. The simulated and measured results of the return loss and insertion loss were S33= -24 dB, S35 = -5.3 dB, S36 = -6.2 dB, S37 = -6.25 dB, S38 = 6.4 dB, and S33= -15 dB, S35 = -5.8 dB, S36 = 6.7 dB, S37 = 6.56 dB, S38 = -7 dB, as shown in Fig. 7 (e-f), The average insertion loss for simulated and measured (S35,S36,S37,S38) were -6.0 ±2 dB, respectively. The P4 of the BM excited return loss was better than 15 dB. The simulated and measured results of the return loss and insertion loss were S44= -20 dB, S45 = -5.4 dB, S46 = -5.18 dB, S47 = -5.0 dB, S48 = -6.19 dB, and S44= -24 dB, S45 = -5.95 dB, S46 = -6.37 dB, S47 = -7.1 dB, S48 = -6.65 dB, as shown in Fig. 7(g-h). The average insertion loss for simulated and measured (S45,S46,S47,S48) were -6.1 ± 2dB, respectively. All the results for P1, P2, P3, and P4 were at centre frequency of 3.5 GHz. The overall results, when P1, P2, P3, and P4 were excited, the simulated and measured proposed design 4 × 4 BM had good agreement between them, although there some variation observed in the results due to the extra loss phase shifts induced by the cable and connector.

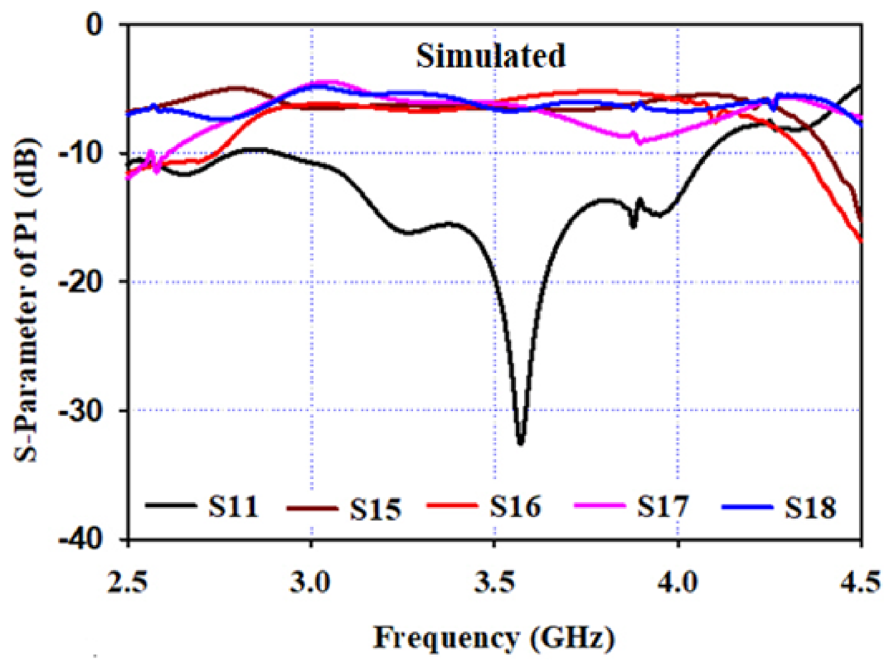

(a)

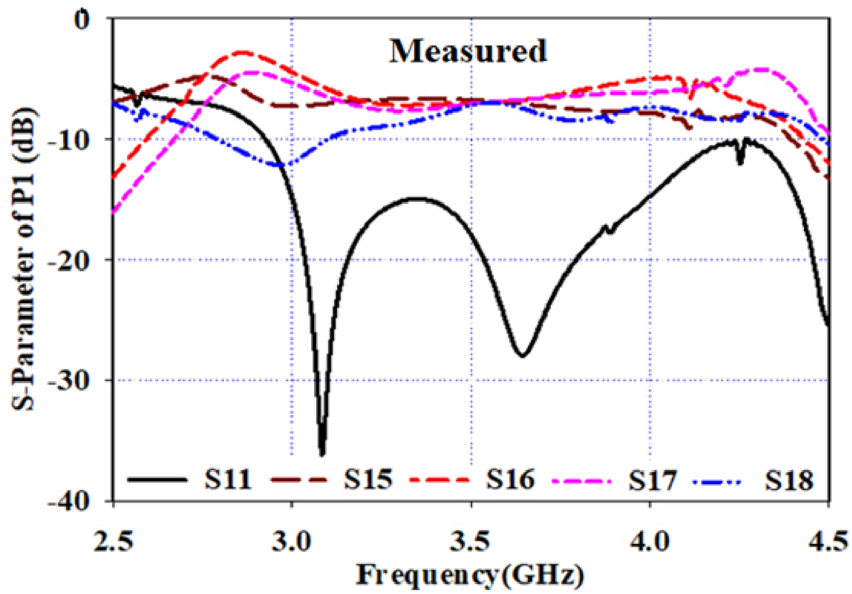
Measured
S-Parameter of P1 (dB)
0
-10
-20
-30
-40
2.5
3.0
3.5
4.0
4.5
Frequency(GHz)
S11
S15
S16
S17
S18

(b)

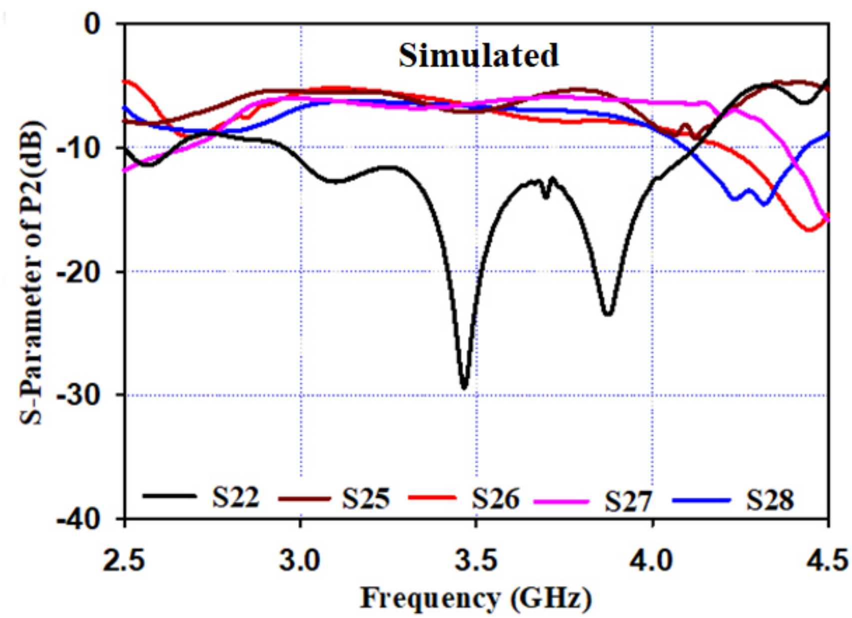
Simulated
S-Parameter of P2(dB)
0
-10
-20
-30
-40
2.5
3.0
3.5
4.0
4.5
Frequency (GHz)
S22
S25
S26
S27
S28

(c)

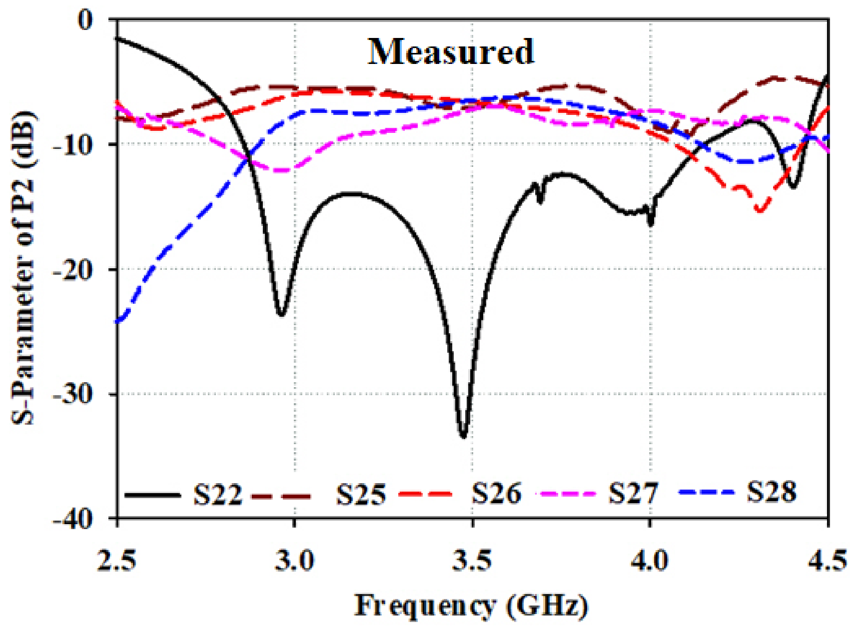
Measured
S-Parameter of P2 (dB)
0
-10
-20
-30
-40
S22
S25
S26
S27
S28
2.5
3.0
3.5
4.0
4.5
Frequency (GHz)

(d)

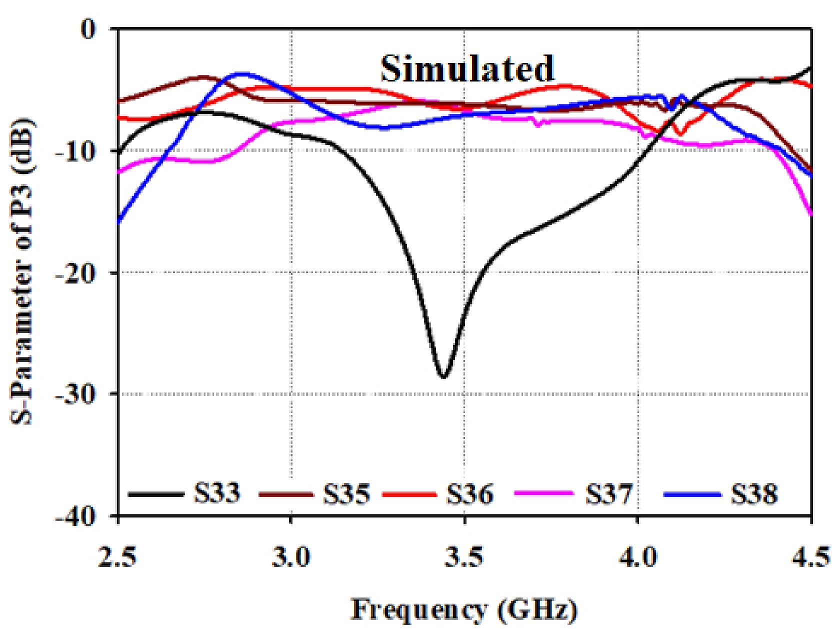
Simulated
S-Parameter of P3 (dB)
0
-10
-20
-30
-40
S33
S35
S36
S37
S38
2.5
3.0
3.5
4.0
4.5
Frequency (GHz)

(e)

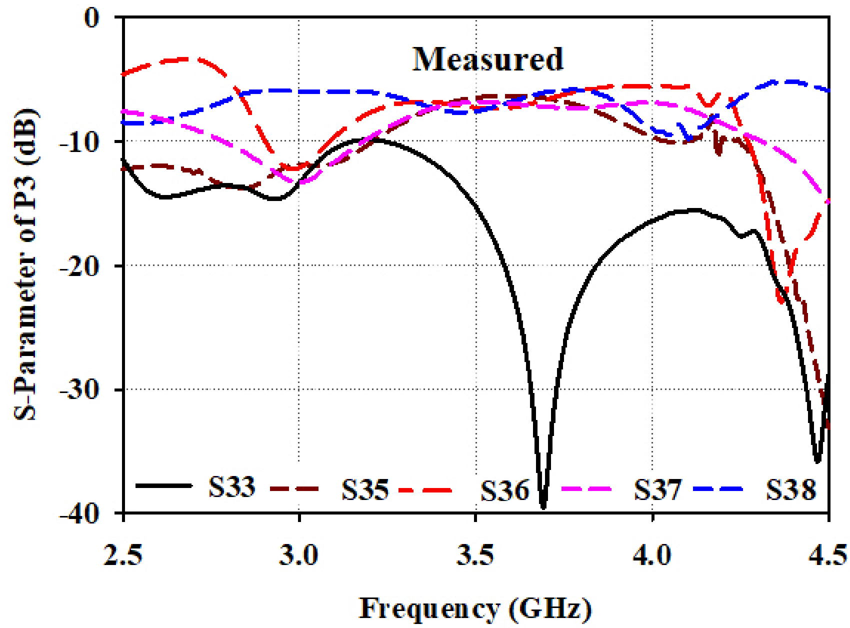
Measured
S-Parameter of P3 (dB)
Frequency (GHz)
S33
S35
S36
S37
S38
0
-10
-20
-30
-40
2.5
3.0
3.5
4.0
4.5

(f)

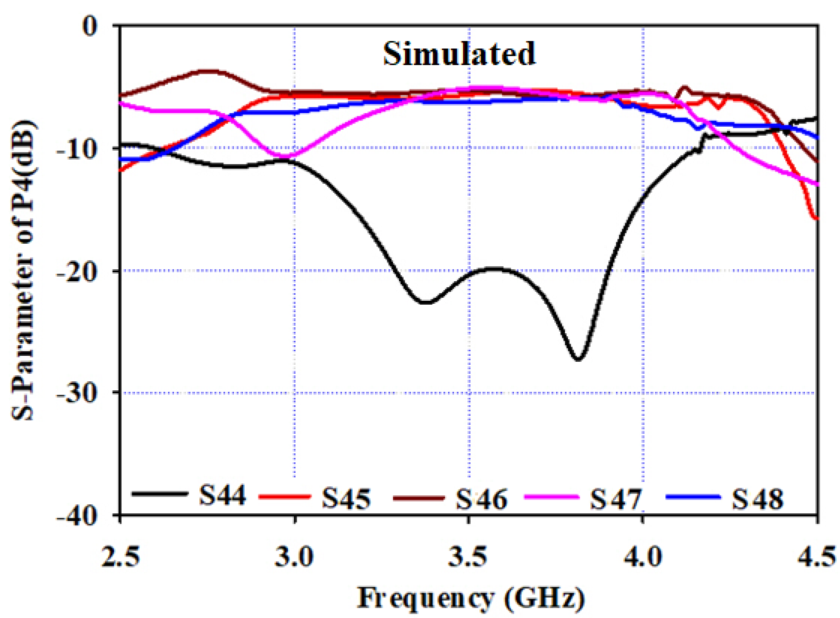
Simulated
S-Parameter of P4(dB)
Frequency (GHz)
S44
S45
S46
S47
S48
0
-10
-20
-30
-40
2.5
3.0
3.5
4.0
4.5

(g)

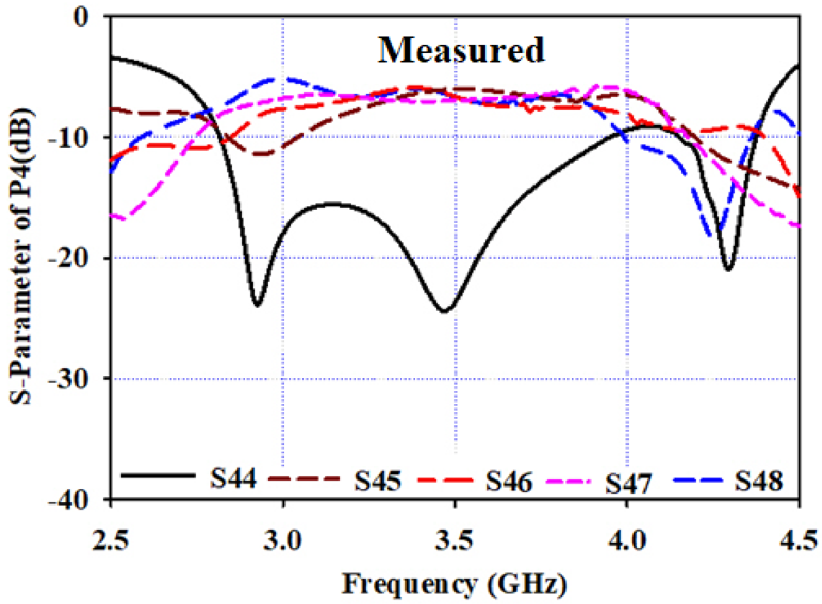

(h)

Fig. 7. Simulated and Measured response of the BM (a-b) for the input P1, (c-d) for the input P2, (e-f) for the input P3, (g-h) for the input P4.

Fig. 8 shows the differences in results between simulated and measured of the phase differences at BM centre frequency of 3.5 GHz. According to the simulated, the phase differences for output at P1 -45°was (S15, S16, S17, S18) -46°, -43.3°, -41.5°. Correspondingly, the measured phase differences were (S15, S16, S17, S18) -47.20, 49.40, 51.10, respectively. So, the errors between output ports were 10, 1.70, 3.50 and 2.20, 4.40, 6.10, which introduced the average errors of 2.00 and 4.20, as shown in Fig. 8 (a-b). However, the quartered phase is as mentioned in Table 4. The phase differences when P2 excited by 1350 were indicated by the simulated as in 1320 between (S26-S25), 1290 between ports (S27 – S26), and 139° between ports (S28 – S27), respectively. Thus, the errors between the output ports 30, 60, and 40 introduced the average errors of 4.30, respectively. The measured phase differences indicated 1280 between ports (S26 - S25), 1420 between ports (S27 – S26), 1400 between ports (S28 – S27) at center frequency, as shown in Fig. 8 (c-d). Hence, the errors were 70,110, and 90, introducing the average errors of 90. The phase difference between simulated and measured results reflected very good agreement, as summarised in Table 4. The output P3 of the BM excited revealed that the adjacent port should be by -1350 per design, as summarised in Table 5. In simulated and measured results, it was that found the phase differences between the output results were -1330,-1380,-1410 and -1420,-1270,-1310, at centre frequency of 3.5 GHz, respectively. These values were different from the desired values by 20, 30, 60 and 70' 80, 40, introducing the average errors of 3.67^0 and 6.330 at operation frequency of 3.5GHz, respectively.

As show in Fig. 8 good performances between simulated and measured results when output P4 excited. Table 4 as summarised the phase difference between adjacent outputs ports should be 45° as per design. For the simulation result, the phase difference was 44^0 between output P5, P6 (S 45 - S 46), 480 between P7, P6 (S 47 -S 46), 400 between P8, P7 (S 48 – S 47), respectively. So, the errors of the simulated result between outputs 10, 30, and 5^0 introduced the average errors of 30, respectively. Meanwhile, the measured result of the phase difference was 500 between output P5, P6 (S45 – S46), 390 between P7, P6 (S47 – S46), 520 between P8, P7 (S48 – S47), respectively, at operate frequency of 3.5GHz. So, the errors of the measured results between outputs 50, 60, and 70 introduced the average errors of 60, respectively. There small error in phase difference between simulated and measured results due to the variation for electrical permittivity parameter, as summarised in Table 5.

The comparison of S-parameters between the simulated and measured 4 × 4 Butler matrix is as illustrated in Fig.9. This comparison between simulated and measured has small difference with loss error due by SAM and coaxial cable show in Fig 9. Tables 3 and Table introduce the summarised simulated and measured results of the BM to the phase difference between the ports and S-parameters of the proposed BM design at centre frequency of 3.5GHz, respectively. From Tables 3 and 4, the phase differences between all of the ports as good agreement with the desired value. As for Table 5, it displays the comparison between the proposed design 4 × 4 BW with the previous work.

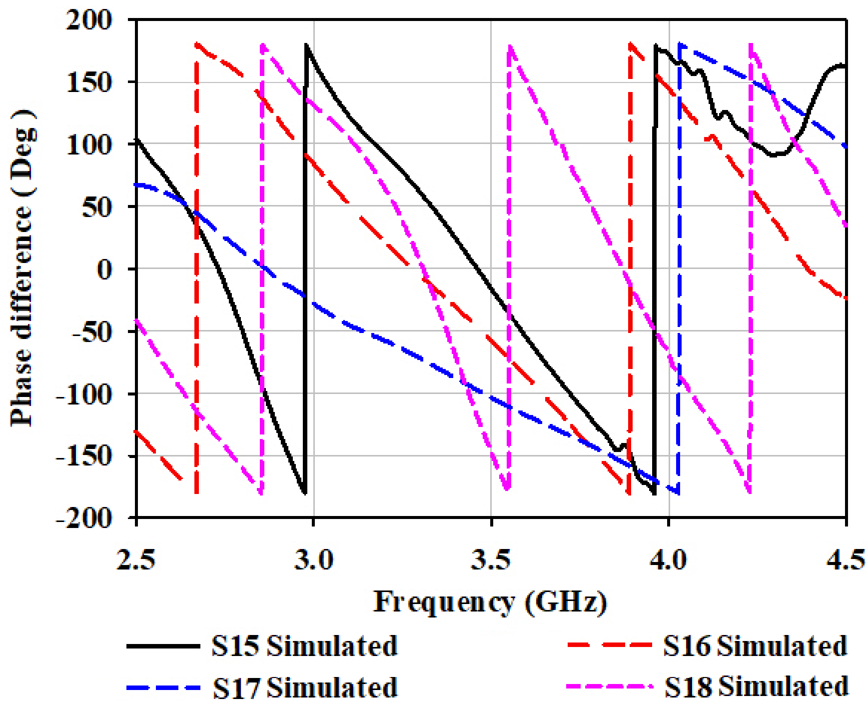

(a)

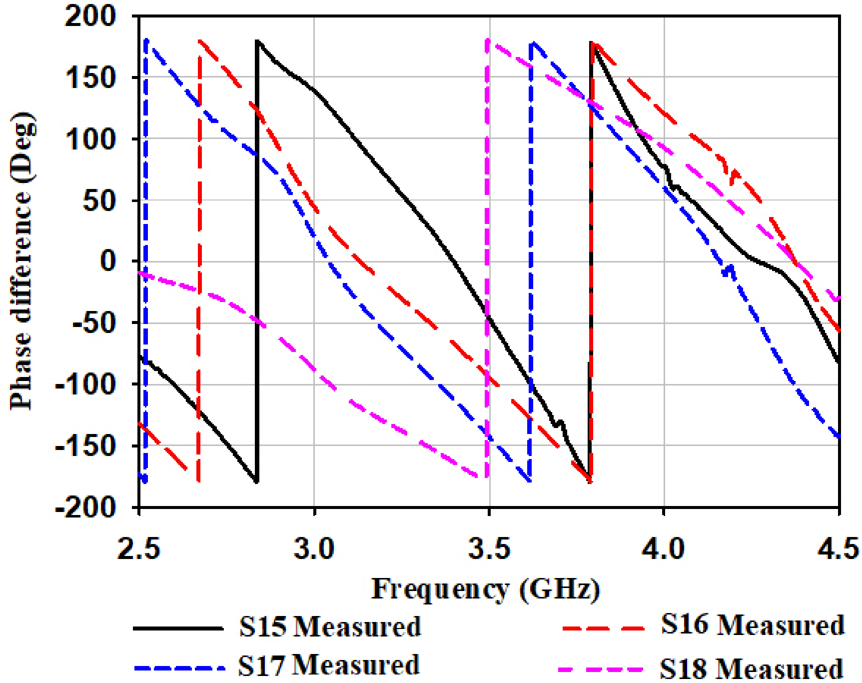
200
150
100
50
0
-50
-100
-150
-200
Phase difference (Deg)
2.5
3.0
3.5
4.0
4.5
Frequency (GHz)
S15 Measured
S16 Measured
S17 Measured
S18 Measured

(b)

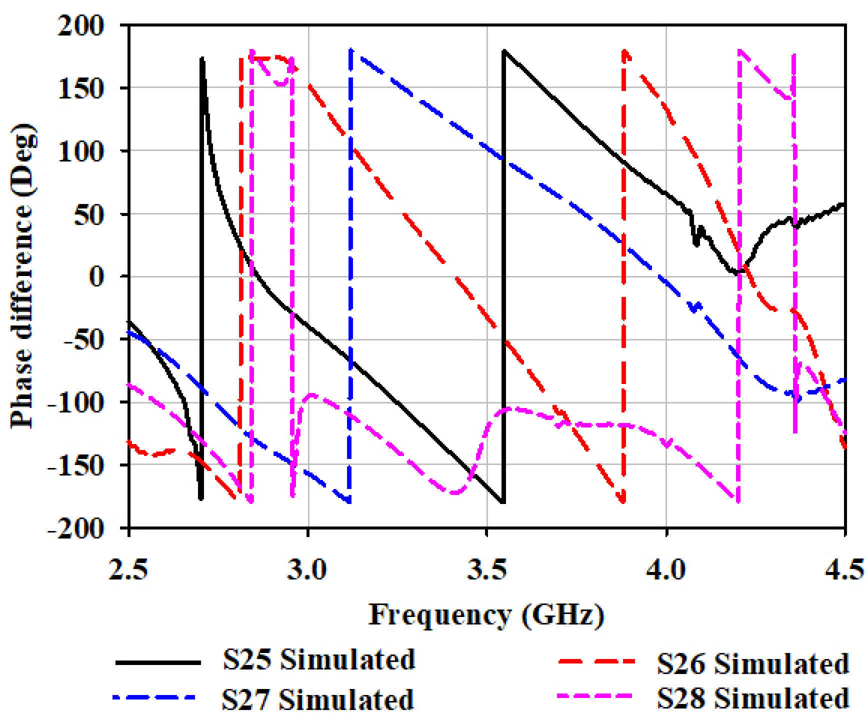
200
150
100
50
0
-50
-100
-150
-200
Phase difference (Deg)
2.5
3.0
3.5
4.0
4.5
Frequency (GHz)
S25 Simulated
S26 Simulated
S27 Simulated
S28 Simulated

(c)

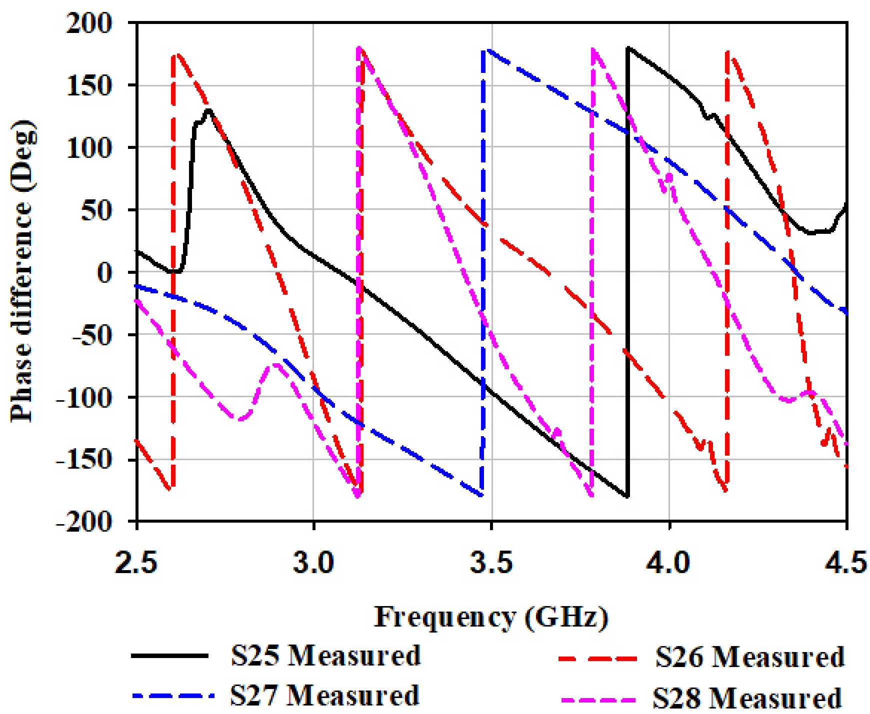
200
150
100
50
0
-50
-100
-150
-200
Phase difference (Deg)
2.5
3.0
3.5
4.0
4.5
Frequency (GHz)
S25 Measured
S26 Measured
S27 Measured
S28 Measured

(d)

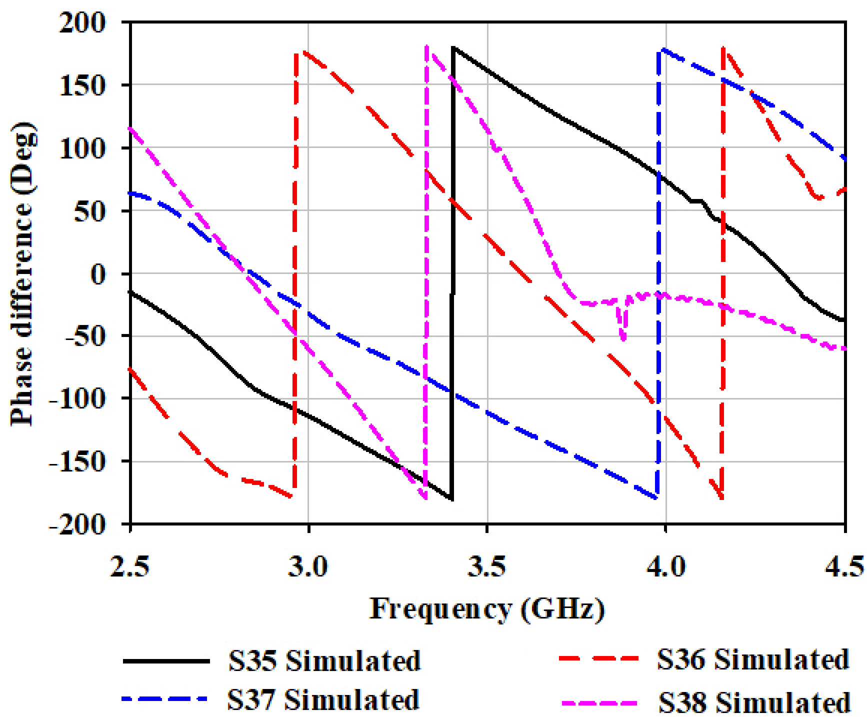
200
150
100
50
0
-50
-100
-150
-200
Phase difference (Deg)
2.5
3.0
3.5
4.0
4.5
Frequency (GHz)
S35 Simulated
S36 Simulated
S37 Simulated
S38 Simulated

(e)

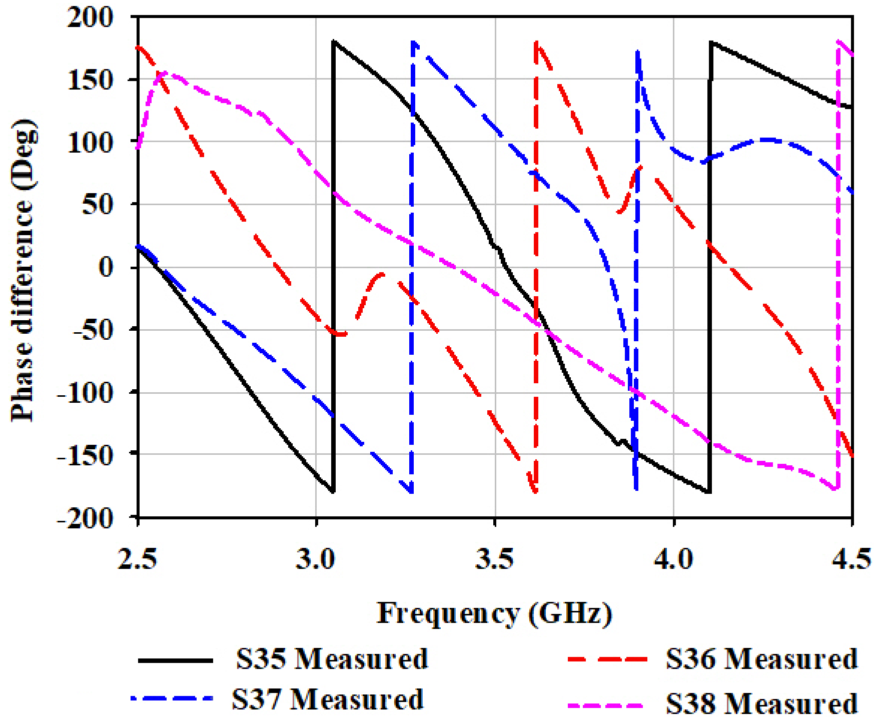

200
150
100
50
0
-50
-100
-150
-200
Phase difference (Deg)
2.5
3.0
3.5
4.0
4.5
Frequency (GHz)
S35 Measured
S36 Measured
S37 Measured
S38 Measured

(f)

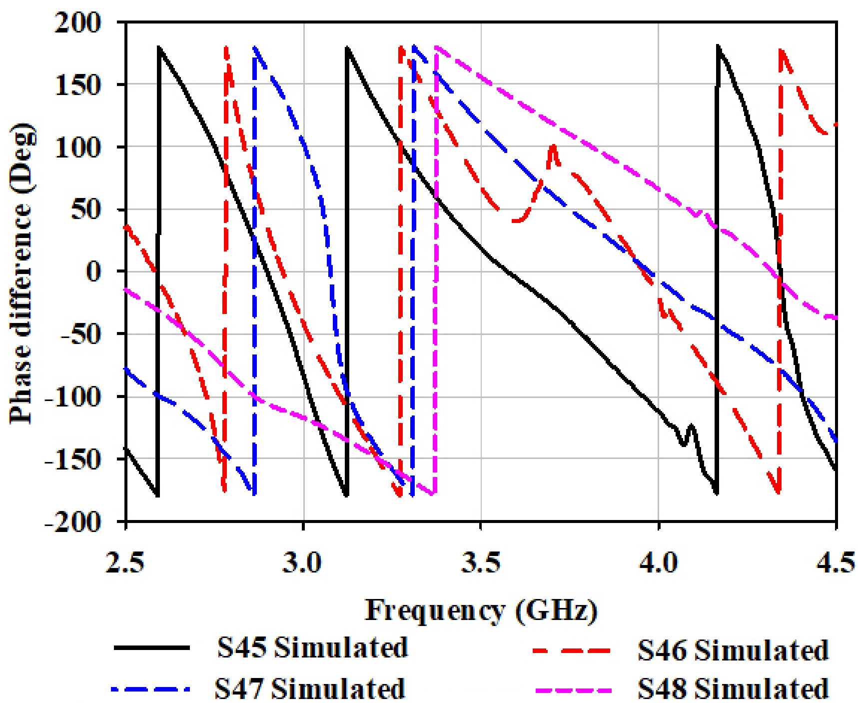

200
150
100
50
0
-50
-100
-150
-200
Phase difference (Deg)
2.5
3.0
3.5
4.0
4.5
Frequency (GHz)
S45 Simulated
S46 Simulated
S47 Simulated
S48 Simulated

(g)

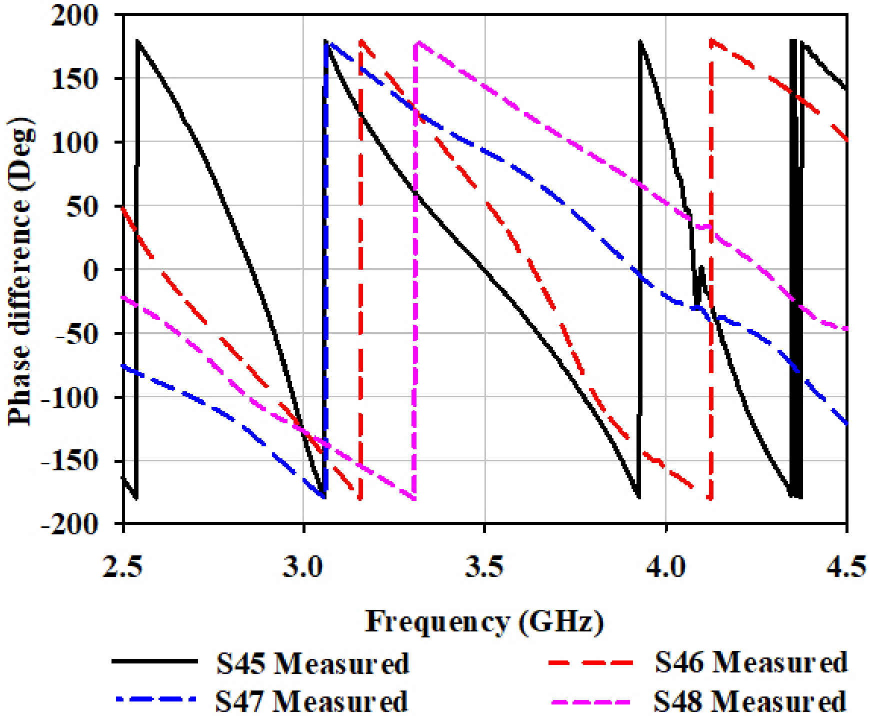

(h)

Fig. 8. Simulated and Measured result of the phase differences output ports, when P1 (-450) is excited, when P2 (1350) is excited, when P3 (-1350) is excited, when P4 (450) is excited.

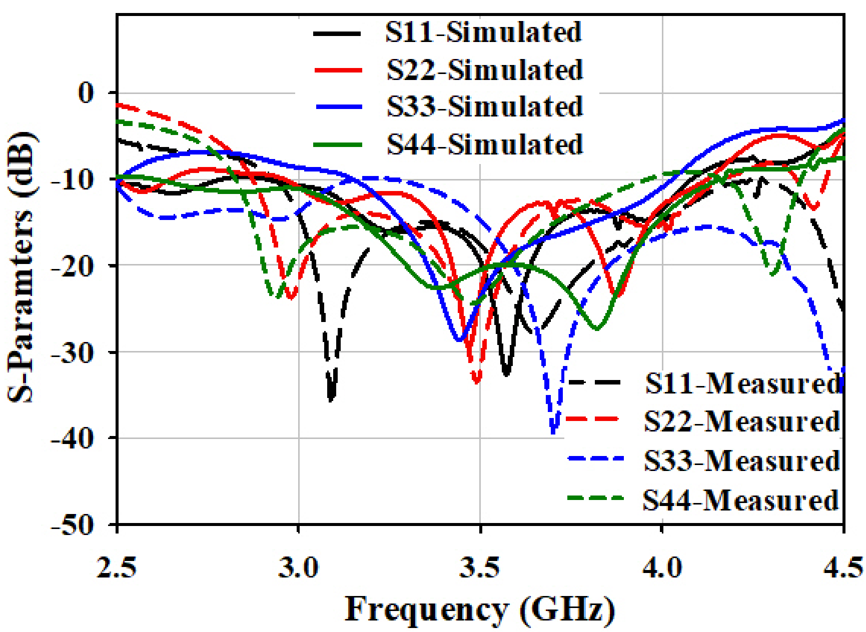

Fig.9. Comparison between simulated and measured S-parameters.

Design switched beamforming antenna array

The switched beamforming antenna array system was based on 4 × 4 BM with 1 × 4 element antenna array. The use of BM is to shift the beam in a different direction; the antenna array connected with BM was presented to develop SAA, as shown in Fig.10. The proposed design of the BM and antenna system operated at centre frequency of 3.5 GHz, respectively. The proposed design 4 × 4 BM have four input and output ports, compact four 3-dB BLC, two crossover structure, and two 45°phase shifters. The use of BM was to shift the beam in different directions. Depending on the input ports (P1, P2, P3, and P4) which fed the output ports to the signal phase (P5, P6, P7, and P8) of the proposed BM, they developed a -45°,+135°, -135°, and +45o phase difference between the output ports. The results of the simulated and measured radiation patterns, obtained by exiting various input ports of the proposed BM, produced four orthogonal beams deposed at -340,320,-400 , and 350, as illustrated in Fig. 10. The four beams steered were 1L, 2R, 2L, and 1R with excited input ports of P1, P2, P3, and P4, respectively.

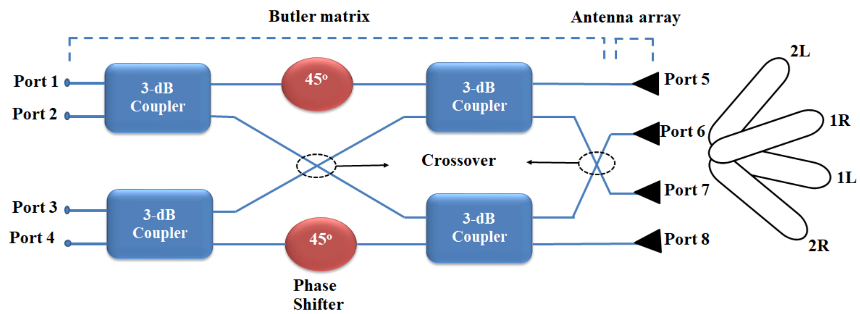

Fig. 10. Block diagram of the antenna array with the 4 × 4 BW.

The microstrip patch antenna design was widely used due the small size, simple structure, and easy fabrication. A microstrip patche antenna operating at 3.5 GHz. After applying the zig-zag structure at resonating frequency to 3.5GHz with simulated a return loss (S11) of -20dB and a bandwidth of 410MHz (3.36GHz-3.77). The zig-zag structure of the antenna have measured return loss -31dB and bandwidth of 460MHz (3.33GHz-3.79GHz) as show in Fig.11 obtained good return loss for the simulated and measured of the single element patch antenna. The back side ground plane was reduced due to the back lobe level. Hence, the BM signal feeding structure to the patch should be carefully designed. Taking this into consideration. We designed and implemented the block level for the 4 × 4 Butler matrix and 1 × 4 patch antenna array, then optimised their performance independently.

In this work, we carefully implemented the Butler matrix overall, the antenna elements, and the interface structures between our extensive co-optimization. Fig. 12 exhibits the proposed design of the beamforming antenna array. The 4 × 4 Butler matrix and 1 × 4 antenna array under tested, in anechoic chamber were printed on the single layer, as illustrated in Fig. 13. The single element of the rectangular patch antenna had the overall size of 16.4 × 16.4 mm2 and the feed line of 1.50 mm was placed with a distance of λ0/2 (λ0) as the wavelength. Due to this, the overall performance of the Butler matrix and the antenna elements' interfacing and interconnecting were likely to be affected. The block diagram of the proposed Butler matrix with antenna array was designed for the 5G application. The substrate chosen was a Rogers RT5880LZ with the thickness of 0.25 mm, dielectric permittivity of 2, and loss tangent of 0.0021, respectively. The inconsistencies may be due to extra losses and phase shifts prompted by the SAM and coaxial cable. From now onwards, discussions relating to the results will be based on the compact structure of the SAA shown in Fig. 14. The radiation pattern measurements of the fabricated SAA are then performed in the anechoic chamber using Rohde & Schwarz ZVL-vector network analyzer (VNA) and horn antenna. The BFN and distance between the antenna elements selected the direction of the main beam radiation, as shown in Fig.14

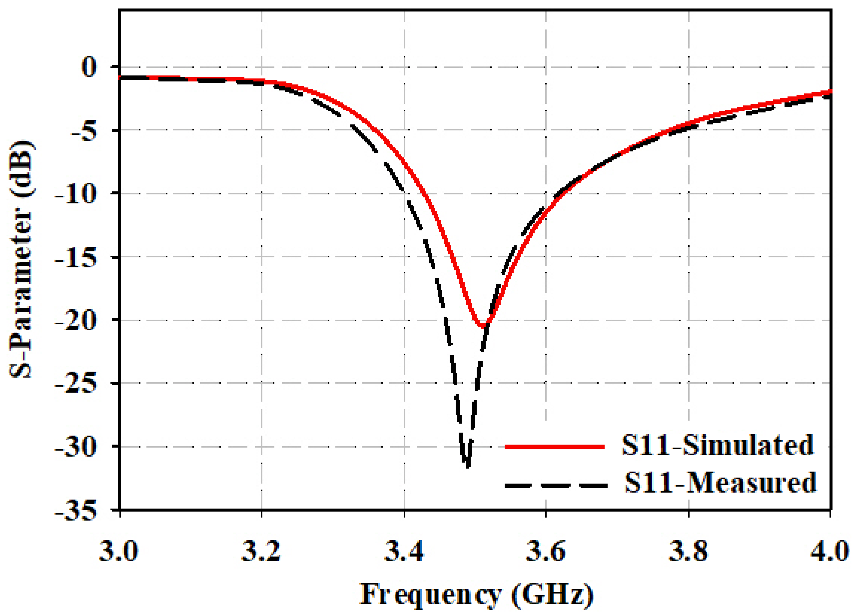

Fig. 11. Return loss of single element patch antenna

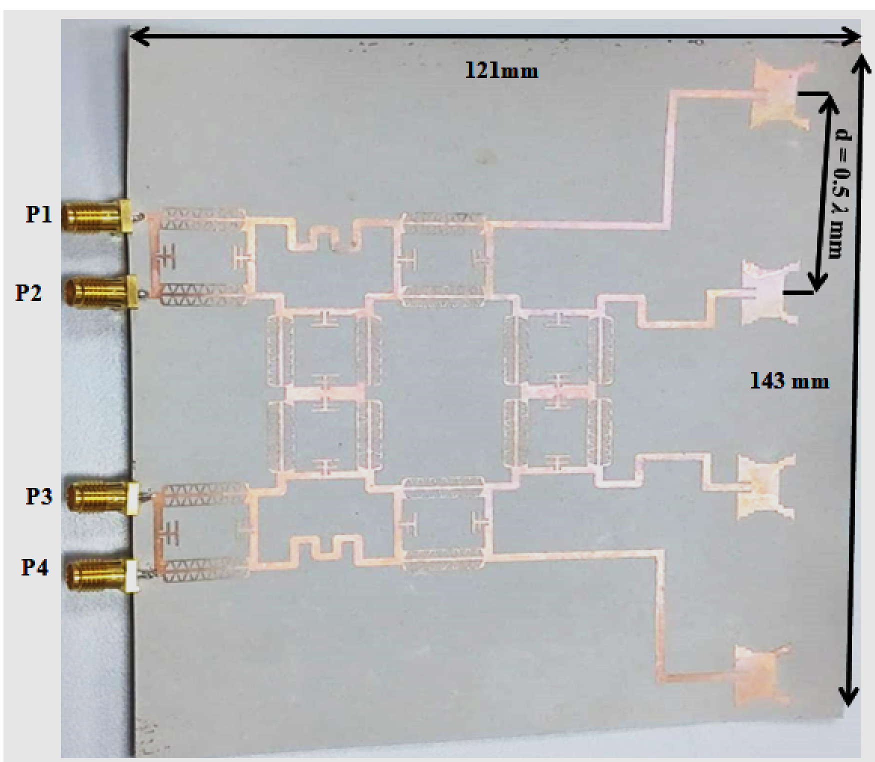

Fig.12. Compact structure of the SAA, the spacing between the antenna elements $d = 0.5\lambda$ Top layer.

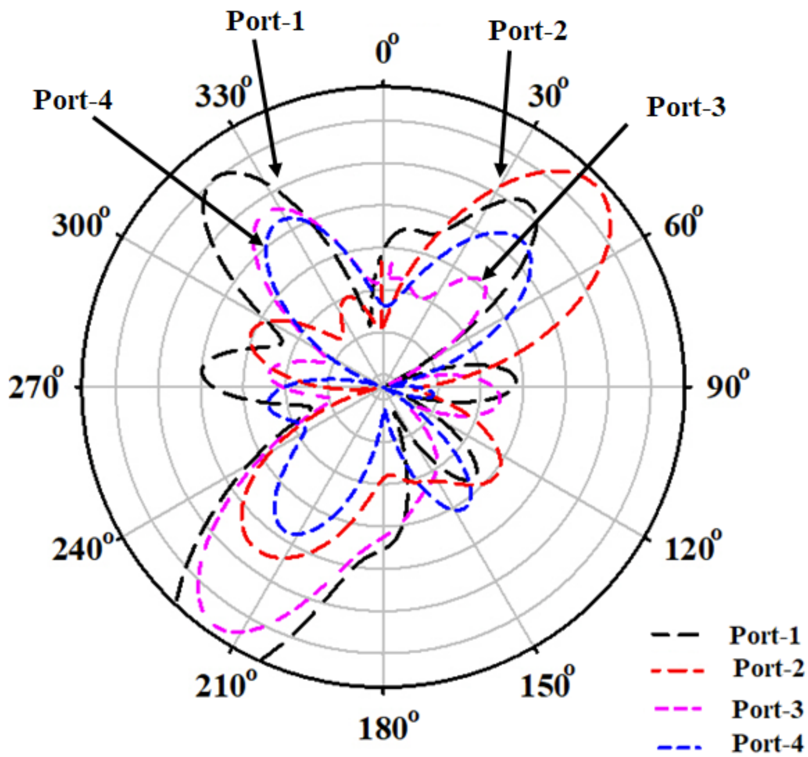
Port-1
Port-2
Port-3
Port-4
0°
30°
60°
90°
120°
150°
180°
210°
240°
270°
300°
330°
Port-1
Port-2
Port-3
Port-4

(a)

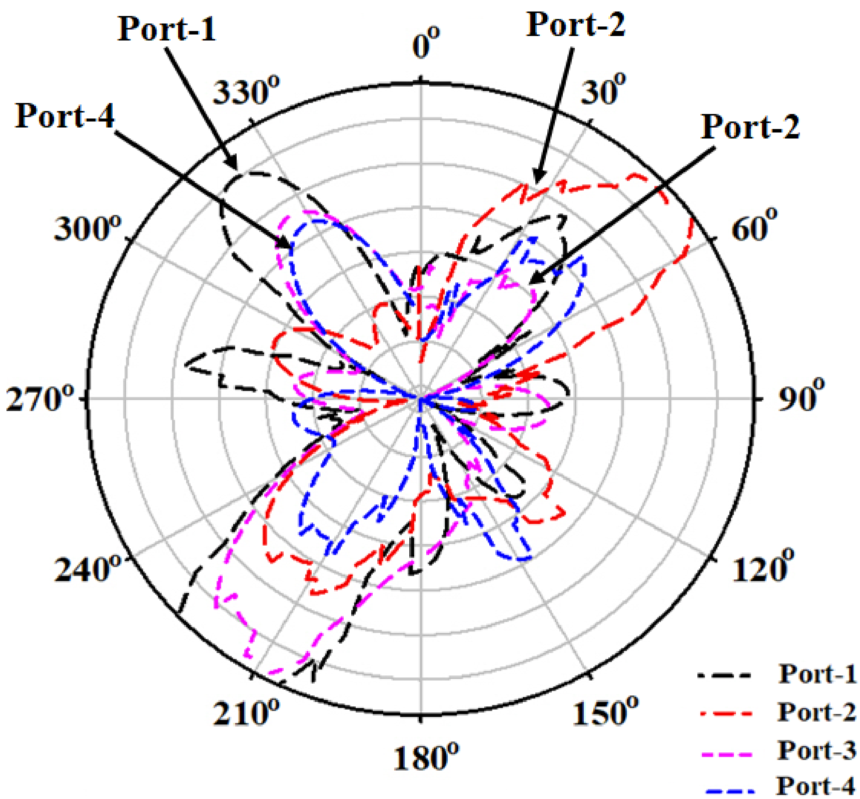

(b)

Fig.13. Radiation pattern results of linear 1×4 antenna array , when each input port of BM are excited (a) Simulated and (b) Measured result, respectively

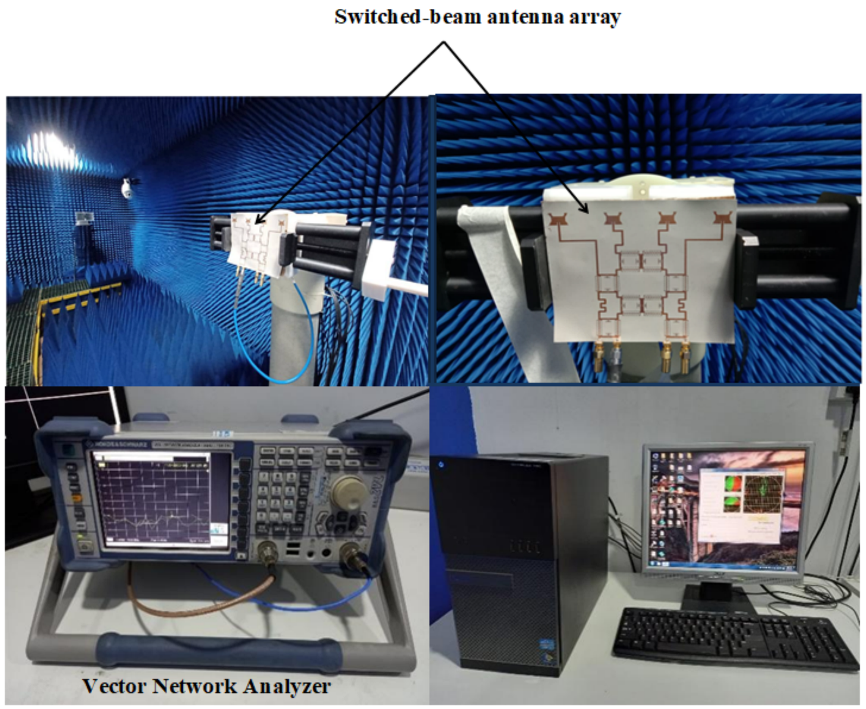
Switched-beam antenna array
Vector Network Analyzer

(a)

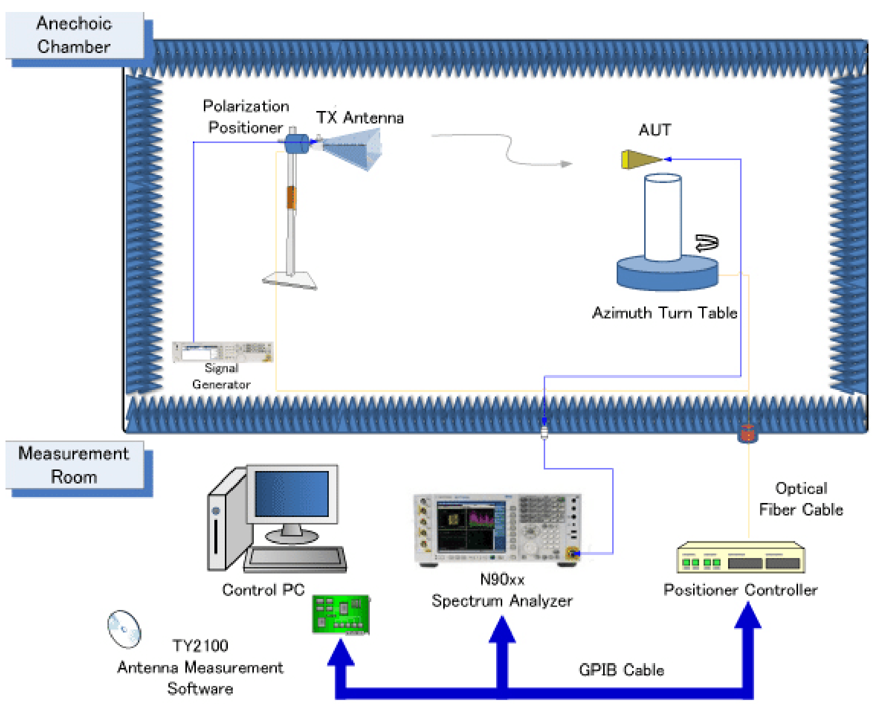
Anechoic Chamber
Polarization Positioner
TX Antenna
AUT
Azimuth Turn Table
Signal Generator
Measurement Room
Optical Fiber Cable
Control PC
N90xx Spectrum Analyzer
Positioner Controller
TY2100 Antenna Measurement Software
GPIB Cable

(b)

Fig. 14. Radiation pattern measurement setup,(a) Butler matrix inside anechoic chamber(b) Block diagram

Table 4. Simulated and measured Phase difference of the proposed design BM at 3.5 GHz.

Ports	**Phase difference between ($P5^0$,$P6^0$)**	**Phase difference between ($P5^0$,$P6^0$)**	**Phase difference between ($P6^0$,$P7^0$)**	**Phase difference between ($P6^0$,$P7^0$)**	**Phase difference between ($P7^0$,$P8^0$)**	**Phase difference between ($P7^0$,$P8^0$)**	**Required phase difference (Deg)**
	Simulatd	**Measured**	**Simulatd**	**Measured**	**Simulated**	**Measured**	
Port 1	-46^0	-47.2^0	-43.3^0	-49.4^0	41.5^0	51.1^0	**-45^0**
Port 2	132^0	128^0	139^0	142^0	139^0	140^0	**135^0**
Port 3	-133	-142	-138	-127	-141	**-131**	**-135^0**
Port 4	44	50	48	39	40	52	**45^0**

Table 5 . Comparison between proposed design BM at 3.5 GHz with previous work

Ref	**Frequency**	**Material**	**Technique**	**Bandwidth**	**Size (mm)**
[24]	3.5	FR-4	Open-circuit coupled line and capacitor unit cell	550	70 × 73.7
[27]	2.4	Rogers 4003C	Circularly polarized (CP)	900	170 × 170
[37]	2.44	FR-4	Without crossover	200	96 × 96
[38]	2.5	FR-4	Open-stub and removal crossover	200	115.18 × 64.4
[39]	2.5	FR-4	Two section branch line coupler	400	120 × 150
[40]	1.8	ARLON	Composite right/left handed CRLH-TL	200	109 × 119
[41]	6	Roger 4003C	Mushroom-like	2300	100 ×110
[42]	0.86	RT/duroid 5880	double spiral lines (SDSLs)	150	109.0 × 89.3
[43]	2.4	Plastic	complimentary square split ring resonators (CS-SRRs)	300	154 × 117
This work 2023	**3.5**	**RT/5880LZ**	**Triangular slot and T-shape**	**836**	**85.5 × 75**

Conclusion

This work presented a 4 × 4 Butler matrix to feed the direction-switched beamforming antenna array for 3.5 GHz 5G wireless application. The desired result was achieved via Computer Simulation Technology (CST). So, the finalised proposed design for BM and antenna array system array was fabricated on single layer

Rogers RT5880LZ. The measured result of the BM and antenna array system showed a good agreement compared to the simulated result, which successfully steered radiation beams of -34°, -40°, +32°, and +35°. The overall size of the antenna and Butler matrix was 121mm × 143mm. The result demonstrated that the proposed four-beam antenna array revealed a good agreement for communication system, as well as beam-forming for 5G wireless application.

Reference

[1] S. Roshani, S. I. Yahya, S. Roshani, and M. Rostami, "Design and Fabrication of a Compact Branch-Line Coupler Using Resonators with Wide Harmonics Suppression Band," *Electron.* , vol. 11, no. 5, pp. 1–19, 2022.

[2] A. A. Abdulbari, S. K. Abdul Rahim, P. J. Soh, M. H. Dahri, A. A. Eteng, and M. Y. Zeain, "A review of hybrid couplers: State-of-the-art, applications, design issues and challenges," *Int. J. Numer. Model. Electron. Networks, Devices Fields* , vol. 34, no. 5, pp. 1–19, 2021.

[3] N. Syahira, M. Suhaimi, N. Muzlifah, and W. Ismail, "Miniaturized 4 × 4 switched-beam switched-beam Butler Matrix with bandwidth enhancement for 5G communication system," *Alexandria Eng. J.* , vol. 61, no. 12, pp. 13089–13103, 2022.

[4] T. S. Rappaport *et al.* , "Wireless communications and applications above 100 GHz: Opportunities and challenges for 6g and beyond," *IEEE Access* , vol. 7, pp. 78729–78757, 2019.

[5] A. A. Abdulbari *et al.* , "New design of wideband microstrip branch line coupler using T-shape and open stub for 5G application," *Int. J. Electr. Comput. Eng.* , vol. 11, no. 2, pp. 1346–1355, 2021.

[6] S. A. Babale, S. K. Abdul Rahim, O. A. Barro, M. Himdi, and M. Khalily, "Single Layered 4 × 4 butler matrix without phase-shifters and crossovers," *IEEE Access* , vol. 6, pp. 77289–77298, 2018.

[7] A. A. Abdulbari *et al.* , "Single-Layer Planar Monopole Antenna-Based Artificial Magnetic Conductor (AMC)," *Int. J. Antennas Propag.* , vol. 2022, 2022.

[8] D. Muirhead, M. A. Imran, and K. Arshad, "A Survey of the Challenges, Opportunities and Use of Multiple Antennas in Current and Future 5G Small Cell Base Stations," *IEEE Access* , vol. 4, no. c, pp. 2952–2964, 2016.

[9] K. Wincza and S. Gruszczynski, "Broadband Integrated 8 x 8 Butler Matrix Utilizing Quadrature Couplers and Schiffman Phase Shifters for Multibeam Antennas With Broadside Beam," *IEEE Trans. Microw. Theory Tech.* , vol. 64, no. 8, SI, pp. 2596–2604, Aug. 2016.

[10] H. Ren, H. Zhang, Y. Jin, Y. Gu, and B. Arigong, "A Novel 2-D 3 X 3 Nolen Matrix for 2-D Beamforming Applications," *IEEE Trans. Microw. Theory Tech.* , vol. 67, no. 11, pp. 4622–4631, 2019.

[11] F. Casini, R. V. Gatti, L. Marcaccioli, and R. Sorrentino, "A novel design method for Blass matrix beam-forming networks," *2007 Eur. Radar Conf. EURAD* , no. October, pp. 232–235, 2007.

[12] K. Tekkouk, M. Ettorre, L. Le Coq, and R. Sauleau, "Multibeam SIW Slotted Waveguide Antenna System Fed by a Compact Dual-Layer Rotman Lens," *IEEE Trans. Antennas Propag.* , vol. 64, no. 2, pp. 504–514, 2016.

[13] H. Ren, B. Arigong, M. Zhou, J. Ding, and H. Zhang, "A Novel Design of 4 × 4 Butler Matrix With Relatively Flexible Phase Differences," *IEEE Antennas Wirel. Propag. Lett.* , vol. 15, no. c, pp. 1277–1280, 2016.

[14] Y. S. Lin and J. H. Lee, "Miniature butler matrix design using glass-based thin-film integrated passive device technology for 2.5-GHz applications," *IEEE Trans. Microw. Theory Tech.* , vol. 61, no. 7, pp. 2594–2602, 2013.

[15] P. Bhowmik and T. Moyra, “Modelling and Validation of a Compact Planar Butler Matrix by Removing Crossover,” *Wirel. Pers. Commun.* , vol. 95, no. 4, pp. 5121–5132, Aug. 2017.

[16] N. A. Muhammad, S. K. A. Rahim, N. M. Jizat, T. A. Rahman, K. G. Tan, and A. W. Reza, “Beam Forming Networks Using Reduced Size Butler Matrix,” *Wirel. Pers. Commun.* , vol. 63, no. 4, pp. 765–784, Apr. 2010.

[17] L. Ma, Y. Wu, and W. Wang, “Design of Wideband Butler Matrix with Equal/Unequal Phase Differences for Flexible Beam-Controllability,” *IEEE Trans. Circuits Syst. II Express Briefs* , vol. 7747, no. c, pp. 2–6, 2021.

[18] Y. Wang, K. Ma, and Z. Jian, “A low-loss butler matrix using patch element and honeycomb concept on SISL platform,” *IEEE Trans. Microw. Theory Tech.* , vol. 66, no. 8, pp. 3622–3631, 2018.

[19] S. Shi *et al.* , “Wideband Planar Phased Array Antenna Based on Artificial Magnetic Conductor Surface,” *IEEE Trans. Circuits Syst. II Express Briefs* , vol. 67, no. 10, pp. 1909–1913, 2020.

[20] L. Markley and G. V. Eleftheriades, “An ultra-compact microstrip crossover inspired by contra-directional even and odd mode propagation,” *IEEE Microw. Wirel. Components Lett.* , vol. 24, no. 7, pp. 436–438, 2014.

[21] A. Imani and M. S. Bayati, “A novel design of compact broadband 4 × 4 Butler matrix-based beam-forming antenna array for C-Band applications,” *AEU - Int. J. Electron. Commun.* , vol. 138, no. July, p. 153901, 2021.

[22] S.-Y. O. and H.-Y. Hwang, “A MINIATURIZED BRANCH-LINE COUPLER USING TRIANGULAR PATCH TYPE ARTIFICIAL TRANSMISSION LINE Song-Yi,” *Microw. Opt. Technol. Lett.* , vol. 55, no. 11, pp. 1718–1721, 2013.

[23] S. A. Babale, S. K. A. Rahim, O. A. Barro, M. Himdi, and M. Khalily, “Single Layered 4 x 4 Butler Matrix Without Phase-Shifters and Crossovers,” *IEEE ACCESS* , vol. 6, pp. 77289–77298, 2018.

[24] A. Karimbu Vallappil, M. K. A. Rahim, B. A. Khawaja, and M. N. Iqbal, “Compact Metamaterial Based 4 × 4 Butler Matrix with Improved Bandwidth for 5G Applications,” *IEEE Access* , vol. 8, pp. 13573–13583, 2020.

[25] T. H. Lin, S. K. Hsu, and T. L. Wu, “Bandwidth enhancement of butler matrix using broadband forward-wave directional coupler and phase difference compensation,” *IEEE Trans. Microw. Theory Tech.* , vol. 61, no. 12, pp. 4099–4109, 2013, doi: 10.1109/TMTT.2013.2288597.

[26] S. Kim, S. Yoon, Y. Lee, and H. Shin, “A miniaturized butler matrix based switched beamforming antenna system in a two-layer hybrid stackup substrate for 5g applications,” *Electron.* , vol. 8, no. 11, 2019, doi: 10.3390/electronics8111232.

[27] and M. F. K. K. T. Chandrasekaran, N. Nasimuddin, A. Alphones, “Compact circularly polarized beam-switching wireless power transfer system for ambient energy harvesting applications,” Int. J. RF Microw. Comput.-Aided Eng. , vol. 29, no. 1, p. e21642, 2019,” *Int. J. RF Microw. Comput* , vol. 29, no. 1, p. 21642, 2019.

[28] C. W. Wang, T. G. Ma, and C. F. Yang, “A new planar artificial transmission line and its applications to aMiniaturized Butler Matrix,” *IEEE Trans. Microw. Theory Tech.* , vol. 55, no. 12, pp. 2792–2801, 2007.

[29] S.-Y. Oh and H.-Y. Hwang, “A slotted triangular-patch type artificial transmission line coupler,” *J Korean Inst Electromagn Eng Sci* , vol. 22, no. 5, pp. 510–515, 2011.

[30] S. Oh, H. Hwang, E. Engineering, and S. Korea, “A MINIATURIZED BRANCH-LINE COUPLER USING TRIANGULAR PATCH,” vol. 55, no. 8, pp. 1718–1722, 2013.

[31] D. M. Pozar, “Microwave Engineering, 3rd ed: John ,Wiley and Sons 2005.”

[32] X. K. Zhang, C. Zhou, G. C. Wu, and Y. Q. Zhuang, "Design of miniaturized branch-line coupler based on novel center-symmetrical spiral-interdigital resonators," *2013 Cross Strait Quad-Regional Radio Sci. Wirel. Technol. Conf. CSQRWC 2013* , pp. 27–30, 2013.

[33] Y. Cao, J. Wen, H. Hong, and J. Liu, "Design of planar dual-band branch-line coupler with π-shaped coupled lines," *Prog. Electromagn. Res. Lett.* , vol. 55, no. August, pp. 113–120, 2015.

[34] A. A. Abdulbari *et al.* , "Design compact microstrap patch antenna with t-shaped 5g application," *Bull. Electr. Eng. Informatics* , vol. 10, no. 4, pp. 2072–2078, 2021.

[35] I. Zahraoui, A. Errkik, J. Zbitou, A. Tajmouati, and A. S. Mediavilla, "A novel design of a fractal antenna for IMT and WiMAX applications," *Int. J. Microw. Opt. Technol.* , vol. 11, no. 6, pp. 428–434, 2016.

[36] H. Zhang, W. Kang, and W. Wu, "A novel compact dual-band branch-line coupler with cross-shaped stubs," *2016 IEEE Int. Conf. Ubiquitous Wirel. Broadband, ICUWB 2016* , pp. 1–4, 2016.

[37] G. A. Adamidis, I. O. Vardiambasis, M. P. Ioannidou, and T. N. Kapetanakis, "Design and implementation of single-layer 4×4 and 8×8 butler matrices for multibeam antenna arrays," *Int. J. Antennas Propag.* , vol. 2019, pp. 1–12, 2019.

[38] P. Bhowmik and T. Moyra, "Modelling and Validation of a Compact Planar Butler Matrix by Removing Crossover," *Wirel. Pers. Commun.* , vol. 95, no. 4, pp. 5121–5132, 2017.

[39] S. Kuwana, H. Hayashi, and R. Ueda, "Simple design of four-element planar butler matrix using two-section branch-line hybrids," *IEEJ Trans. Electr. Electron. Eng.* , vol. 12, pp. S187–S188, 2017.

[40] H.-X. Xu, G.-M. Wang, and X. Wang, "Compact Butler matrix using composite right/left handed transmission line," *Electron. Lett.* , vol. 47, no. 19, pp. 1081–1082, Sep. 2011.

[41] R. K. M. Lou, M. Naser-Moghadasi, and R. A. Sadeghzadeh, "Broadband Planar Aperture-Coupled Antenna Array for WLAN and ITS Beam-Steering Applications," *RADIO Sci.* , vol. 53, no. 2, pp. 200–209, Feb. 2018, doi: 10.1002/2016RS006155.

[42] M. X. Du and H. X. Peng, "Ultra-compact electromagnetic metamaterial transmission line and its application in miniaturized butler matrix," *Prog. Electromagn. Res. C* , vol. 55, no. January, pp. 187–197, 2014.

[43] O. A. Safia, M. Nedil, M. C. E. Yagoub, and W. Yusuf, "Optically transparent compact 4 × 4 Butler matrix for Wi-Fi applications," *Prog. Electromagn. Res. Lett.* , vol. 58, no. October 2015, pp. 119–124, 2016.